INSTITUTE OF PHYSICS PUBLISHING JOURNAL OF PHYSICS: CONDENSED MATTER

J. Phys.: Condens. Matter **14** (2002) R79–R117 PII: S0953-8984(02)17811-8

TOPICAL REVIEW

Predicting phase equilibria in polydisperse systems

Peter Sollich

Department of Mathematics, King's College London, Strand, London WC2R 2LS, UK

E-mail: peter.sollich@kcl.ac.uk

Received 18 September 2001, in final form 27 November 2001
Published 21 December 2001
Online at stacks.iop.org/JPhysCM/14/R79

Abstract

Many materials containing colloids or polymers are polydisperse: they comprise particles with properties (such as particle diameter, charge, or polymer chain length) that depend continuously on one or several parameters. This review focuses on the theoretical prediction of phase equilibria in polydisperse systems; the presence of an effectively infinite number of distinguishable particle species makes this a highly non-trivial task. I first describe qualitatively some of the novel features of polydisperse phase behaviour, and outline a theoretical framework within which they can be explored. Current techniques for predicting polydisperse phase equilibria are then reviewed. I also discuss applications to some simple model systems including homopolymers and random copolymers, spherical colloids and colloid–polymer mixtures, and liquid crystals formed from rod- and plate-like colloidal particles; the results surveyed give an idea of the rich phenomenology of polydisperse phase behaviour. Extensions to the study of polydispersity effects on interfacial behaviour and phase separation kinetics are outlined briefly.

1. Introduction and scope

Statistical mechanics was originally developed for the study of large systems of identical particles such as atoms and small molecules. However, many materials of industrial and commercial importance which contain colloidal particles or polymers do not fit neatly into this framework. For example, the particles in a colloidal suspension are never precisely identical to each other, but have a range of radii (and possibly surface charges, shapes, etc). Industrially produced polymers always contain macromolecules with a range of chain lengths; and hydrocarbon mixtures occurring in the petrochemical industry often consist of a large number of different molecular species best described as having continuously varying properties across each family of molecules. All these materials are therefore *polydisperse*: they contain particles with properties depending continuously on one or several parameters.

In this review, I will focus on the effects of polydispersity on *phase behaviour*: to process a colloidal or polymeric material, one needs to know under which conditions of pressure

and temperature it will be stable against demixing, how many phases will result if it does demix, and what their properties are. The emphasis will be on the problem of predicting such phase behaviour theoretically, although I will complement this by references to experimental observations and the results of computer simulations where appropriate. I will concentrate almost exclusively on *bulk phase equilibria*, giving only the briefest outlook towards the treatment of inhomogeneous systems (interfacial behaviour, etc) and the challenging topic of phase separation kinetics in section 5. Finally, I will only discuss the case of *fixed polydispersity*, where the polydisperse attribute of each particle remains fixed once and for all. This includes all the examples given above; the length of a polymer molecule or the size of a colloidal particle, for example, do not change over time. The contrasting case of variable polydispersity is exemplified by a surfactant solution in which the surfactant molecules form worm-like micelles whose lengths constantly change due to scission and recombination [1]. Systems of this kind have been treated theoretically (see e.g. [2–4] for a recent example) but will be excluded below because their phase behaviour is much less complex than that of systems with fixed polydispersity; the reasons for this are explained in section 2.

In this review, I will first explain why polydisperse phase equilibria are challenging to predict, describe some of the new effects that can occur, and outline a theoretical framework within which they can be explored (section 2). Then I will give an overview of some current techniques for predicting polydisperse phase equilibria (section 3). Applications to some simple model systems are discussed in section 4, with the aim of giving an idea of the rich phenomenology of polydisperse systems. Section 5 describes briefly the considerable challenges that one faces when looking at polydispersity effects on interfacial behaviour and phase separation kinetics.

Because of the volume of the literature, I will not attempt to give a historical account of the development of theoretical work on polydisperse phase behaviour. The following, very selective, sketch will have to suffice: de Donder's work in the 1920s on many-component mixtures [5] is often cited as an early and important precursor. From the 1940s onwards, there were significant contributions in the area of polydisperse (homo- and co-)polymers, associated with the names of Flory, Huggins, Koningsveld, Scott, Solc, and Staverman [6–13] among many others. Around the same time, the concept of polydispersity also appeared in the treatment of the distillation of multi-component hydrocarbon mixtures (see e.g. [14, 15]). Since then polydispersity has been recognized as important in many other contexts, notably the phase behaviour of suspensions of spherical [16, 17] and non-spherical (e.g. rod-like [18]) colloidal particles.

2. Polydisperse phase equilibria

2.1. The challenge

To understand why the prediction of phase equilibria in polydisperse systems is a challenging problem, it is useful to recall first the procedure for a monodisperse system. In a suspension of identical colloidal particles, for example, the experimentally controlled variables would be the temperature T, the suspension volume V, and the number N of colloidal particles; the appropriate thermodynamic ensemble is therefore the canonical one, and the thermodynamic potential is the Helmholtz free energy $F(N, V, T)$. Here I assume (and will do so throughout in what follows) that the solvent degrees of freedom have been formally eliminated, so that F includes the effects of the solvent only through any effective interaction it may mediate between the colloids. The suspension will separate into two phases with particle numbers $N^{(\alpha)}$ and volumes $V^{(\alpha)}$ ($\alpha = 1, 2$) if it can thereby lower its total free energy $\sum_\alpha F(N^{(\alpha)}, V^{(\alpha)}, T)$

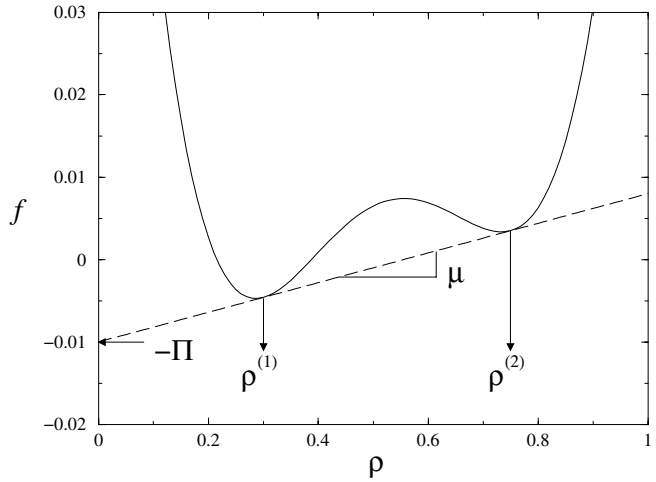

Figure 1. The double-tangent construction for finding phase equilibria (for monodisperse systems). Shown is a sketch of a free energy density f versus particle density ρ (solid curve) and the double tangent to it (dashed line). The tangency points identify the densities $\rho^{(1)}$ and $\rho^{(2)}$ of the coexisting phases. The slope and the negative intercept of the tangent give the chemical potential μ and the osmotic pressure Π, respectively; both are common to the coexisting phases. A parent phase with a density intermediate between $\rho^{(1)}$ and $\rho^{(2)}$ will phase separate into two phases with these densities, thereby lowering the total free energy of the system.

below the value $F(N, V, T)$. The $N^{(\alpha)}$ and $V^{(\alpha)}$ adopt the values which minimize this total free energy, subject to conservation of volume ($\sum_\alpha V^{(\alpha)} = V$) and particle number ($\sum_\alpha N^{(\alpha)} = N$). Introducing Lagrange multipliers for these constraints then gives the familiar coexistence conditions of equal chemical potential $\mu = \partial F/\partial N$ and pressure $\Pi = -\partial F/\partial V$ in the two phases. (Because of the elimination of the solvent degrees of freedom, Π is actually the osmotic pressure of the colloids, rather than the total suspension pressure.)

Since the free energy is extensive, it can be written as $F(N, V, T) = Vf(\rho, T)$ where $\rho = N/V$ is the (number) density of colloids. In terms of the free energy *density* $f(\rho, T)$, the coexistence condition has a simple geometrical interpretation. From the definition of f, one has $\mu = \partial(Vf(N/V, T))/\partial N = \partial f/\partial\rho$ and

$$\Pi = -\frac{\partial}{\partial V}(Vf(N/V, T)) = -f + \rho\,\partial f/\partial\rho = -f + \mu\rho \tag{1}$$

(the latter result can also be seen directly from the Gibbs–Duhem relation $F + \Pi V - \mu N = 0$). Plotting f as a function of ρ as in figure 1, one sees that μ gives the slope of the tangents to the plot at the densities of the two coexisting phases, and that $-\Pi$ is their intercept with the f-axis. Since μ and Π are equal, so are the tangents themselves: the densities $\rho^{(1)}$ and $\rho^{(2)}$ of the coexisting phases are determined by constructing a *double tangent* to $f(\rho, T)$ (see e.g. [19]). From these densities one can then find the fraction of the system volume $v^{(\alpha)} = V^{(\alpha)}/V$ occupied by each phase, by using particle conservation: dividing $\sum_\alpha N^{(\alpha)} = N$ by V one has $\sum_\alpha (V^{(\alpha)}/V)(N^{(\alpha)}/V^{(\alpha)}) = N/V$ or $\sum_\alpha v^{(\alpha)}\rho^{(\alpha)} = \rho$; for two phases, using $v^{(1)} + v^{(2)} = 1$, this gives the well-known 'lever rule' $v^{(1)} = (\rho - \rho^{(2)})/(\rho^{(1)} - \rho^{(2)})$.

Moving towards the polydisperse case, assume now that there are M different species of colloid particles, each with its own particle number N_i and corresponding density $\rho_i = N_i/V$. All densities are conserved, so

$$\sum_\alpha v^{(\alpha)}\rho_i^{(\alpha)} = \rho_i \tag{2}$$

if the system separates into several phases. The free energy density $f(\{\rho_i\})$ is now a function of all M densities, as well as the fixed temperature T which I suppress from now on in the notation. (I will also call f simply the free energy rather than the free energy density where no misunderstanding is possible.) A plot of $f(\{\rho_i\})$ against the densities ρ_i would give a (hyper-)surface in a graph with $M + 1$ coordinate axes, and to find phase coexistences we would have to construct multiple tangent (hyper-)planes to this surface. Where such tangent planes exist, the total free energy is lowered by phase separation into the appropriate number of phases (which, from Gibbs' phase rule, can be between two and $M + 1$). The densities $\rho_i^{(\alpha)}$ in the different phases are given by the points where the tangent plane touches the free energy surface, and the fractional phase volumes $v^{(\alpha)}$ follow from the conditions (2) together with $\sum_\alpha v^{(\alpha)} = 1$.

Now consider the fully polydisperse case. Let σ be the polydisperse attribute of the particles, e.g. the particle diameter in spherical colloids or the chain length in polymers. To fully describe the composition of the system we now need a *density distribution* $\rho(\sigma)$, defined such that $\rho(\sigma)\,\mathrm{d}\sigma$ is the density of particles with σ-values in the range $[\sigma, \sigma + \mathrm{d}\sigma]$. Formally, this corresponds to a scenario with an infinite number of particle species, as can be seen by splitting the range of σ into M 'bins', defining the ρ_i to be the densities within each bin, and then taking $M \to \infty$ (see e.g. [20]). The tangent plane procedure for finding phase coexistences then clearly becomes unmanageable, both conceptually and numerically: one would have to work in an infinite-dimensional space—which mathematically corresponds to the fact that the free energy becomes a *functional* $f([\rho(\sigma)])$ of the density distribution $\rho(\sigma)$—and Gibbs' phase rule allows the coexistence of arbitrarily many thermodynamic phases.

In summary, then, the challenge in predicting polydisperse phase equilibria arises from the effectively infinite number of conserved densities. This renders the standard approaches developed for mixtures with a finite number of species useless. Note that the difficulty that I am talking about here is that of determining the phase equilibria from a free energy (functional) which is assumed *known*. The calculation of this free energy (or at least of a good approximation to it) is a different—and no less challenging—problem that I will not address in this review. So, in what follows, I will regard each model free energy as given, and do *not* discuss in detail the issue of how good a description of the real system it offers, nor how or whether it can be derived from an underlying microscopic Hamiltonian. Whenever I refer to 'exact' results, I mean the exact thermodynamics of such a model as specified by its free energy.

Finally, having established the presence of an infinite number of conserved densities as the principal obstacle in the prediction of polydisperse phase behaviour, one easily sees why *variable* polydispersity is so much easier to deal with: there, one normally fixes the ratios of the densities ρ_i of the various species to each other in the low-density limit [2,3]. (In the fully polydisperse case this corresponds to fixing in the same limit the shape, but not the overall scale, of the density distribution $\rho(\sigma)$.) However, in this limit the densities are directly related to the chemical potentials, and so one is effectively fixing all chemical potential differences. The thermodynamic variables are then N, V, T and the chemical potential differences, and so there is only a *single* conserved density, just as in the monodisperse case. So, while the actual determination of the relevant (semi-grandcanonical) free energy function might still be a challenging problem, once this function is found the determination of the phase behaviour can proceed by a standard double-tangent construction, and Gibbs' phase rule remains the same as for a monodisperse system.

2.2. Polydispersity gives rich phase behaviour

To try to understand the qualitative features of polydisperse phase behaviour, it is useful to consider first a bidisperse system (with two particle species), for which it is still possible

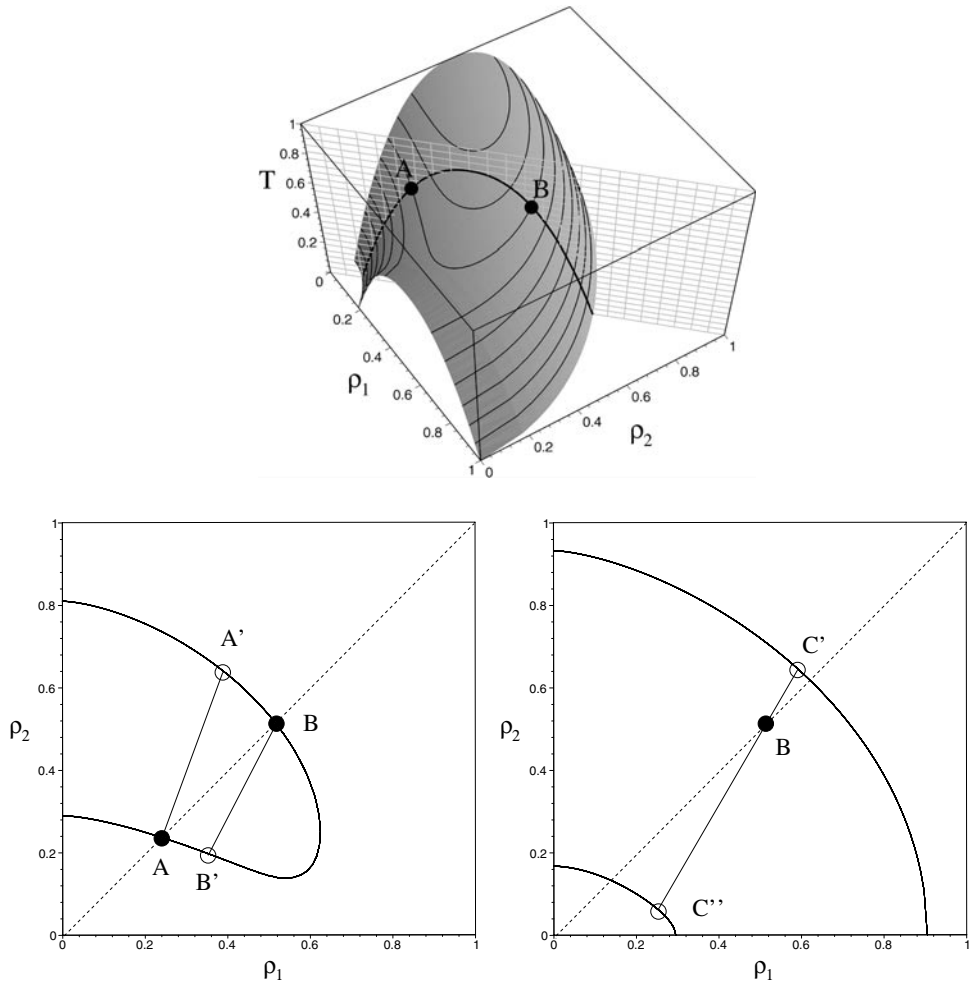

Figure 2. Top: a schematic phase diagram for a bidisperse system. The surface shown in this ρ_1–ρ_2–T plot delimits the region where phase separation into two phases occurs. The vertical plane corresponds to systems on a 'dilution line', for which the composition is fixed (here: the same number of particles of species 1 and species 2) but the overall density can vary. The intersection of this plane with the phase boundary gives the cloud curve shown in figure 3. Bottom left: a horizontal cut through the phase diagram, corresponding to a fixed value T_1 of the temperature. The dashed line is the dilution line. The filled circles, marking the points where the dilution line intersects the phase boundary, give the densities (ρ_1, ρ_2) in the cloud phases, which by definition begin to phase separate at the given temperature T_1. Tie lines connect the cloud phases with the coexisting shadow phases (empty circles); these have different compositions from the cloud phases since they are not located on the dilution line. Bottom right: the situation for a lower temperature T_2. Phase B, which at T_1 had separated off an infinitesimal amount of B′, has now separated into two phases C′ and C″ which are both present in non-zero amounts; neither of them has the same composition as B.

to represent the full ρ_1–ρ_2–T phase diagram graphically. A schematic example of such a phase diagram—inspired by the phenomenology of binary liquids—is shown in figure 2, with some tie lines drawn that connect coexisting phases. (A nice illustration based on the Flory–Huggins theory of polymer solutions is given in [21].) Assume the overall densities of the two particles species are $\rho_1^{(0)}$ and $\rho_2^{(0)}$; I use the '(0)' superscript here to distinguish the properties

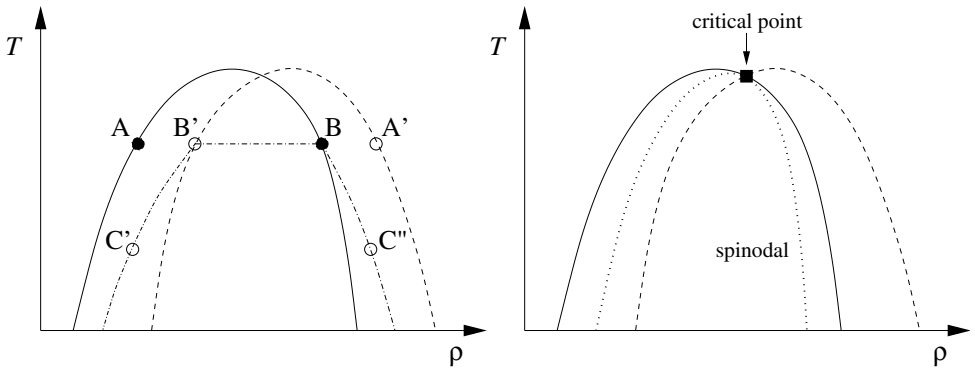

Figure 3. Left: cloud (solid) and shadow (dashed) curves, schematically drawn for the phase diagram of figure 2. On the x-axis is the total particle number density $\rho = \rho_1 + \rho_2$; points corresponding to those in figure 2 are labelled with the same letters. The dash–dotted curves are the coexistence curves for the parent phase B, giving the densities of the phases into which B separates as the temperature is decreased. Right: the spinodal curve and critical point for the same phase diagram. The critical point lies at an intersection of the cloud and shadow curves; the spinodal (dotted) lies inside the cloud curve and touches it at the critical point.

of this 'parent' phase from other generic values of ρ_1 and ρ_2. At high temperatures, the given composition of the system will be stable as a single phase. As T is lowered, however, the system will eventually become able to reduce its total free energy by separating into several (in this case: two) phases. The first temperature where this happens defines the so-called 'cloud point'. At this point, the parent coexists with an infinitesimal amount of a new phase, called the 'shadow' phase [10, 11]. One can repeat this procedure of finding the onset of phase coexistence for a different parent, obtained by diluting with additional solvent; this just changes the total density $\rho_1^{(0)} + \rho_2^{(0)}$ but preserves the ratio of the densities of the two species. Plotting the cloud point temperature against the total parent (cloud phase) density and against the total density of the shadow, for a series of such diluted parents, one obtains the so-called cloud curve and shadow curve, respectively (figure 3). In a monodisperse system, these two curves would coincide, with a critical point at the maximum. In the bidisperse (and more generally the polydisperse) case, however, the cloud point and shadow curve are different, and the critical point occurs at a crossing of the two curves.

To understand this difference between monodisperse and polydisperse systems, it is useful to bear in mind that the set of parent phases whose behaviour is represented by the cloud curve have values of ρ_1 and ρ_2 which lie on a line through the origin in the ρ_1–ρ_2 plane. At a given temperature, the cloud point phases are found as the intersections of this 'dilution line' with the boundaries of the region where phase coexistence occurs, while the corresponding shadow phases are given by the opposite ends of the tie lines starting at the cloud point phases (see figure 2). In general, the shadows therefore do not lie on the dilution line; compared to the dilution line composition which all cloud phases share, the shadow phases have become enriched in one or the other of the two species, a process normally referred to as 'fractionation'. Thus, in contrast to the case for a monodisperse system, the roles of cloud and shadow phases cannot be reversed, and cloud and shadow curves are therefore in general different. The fact that the critical point is located at a crossing of the cloud and shadow curves (rather than at their maximum) follows because at criticality cloud and shadow are by definition identical.

It is also sometimes useful to consider spinodals in a polydisperse system; these are the points where (as temperature is varied, for example) a given parent phase first becomes unstable to local density fluctuations. Determining the spinodal points for all parents on a dilution line

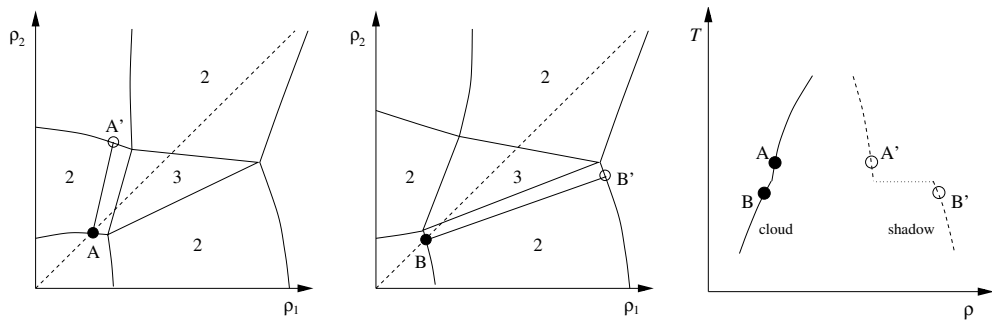

Figure 4. Left and middle: constant-temperature slices through the phase diagram of a bidisperse system, with two- and three-phase regions as indicated. On the left, the dilute cloud phase A (solid circle) begins to phase separate by splitting off a denser phase A′ containing predominantly particles of species 2. On changing T (middle plot), the corner of the three-phase triangle may pass through the dilution line (dashed); at this point, the cloud phase is at a triple point and the properties of the shadow phase change discontinuously, here to a dense phase B′ richer in particles of species 1. Right: schematic cloud and shadow curves for this situation, showing the jump in the shadow curve at the triple point. The cloud curve must be continuous but generally has a kink at the triple point, where it switches between different branches corresponding to separate two-phase regions in the phase diagram.

gives a spinodal curve which can be plotted along with the cloud and shadow curves. By construction, outside the cloud curve single phases are stable against phase separation, so the spinodal curve must lie inside the cloud curve; the critical point always lies on the spinodal curve (since the shadow phase there can be generated by an infinitesimally small fluctuation) and so the spinodal and the cloud curve touch there (see figure 3).

Beyond the onset of phase coexistence, polydisperse phase behaviour becomes yet more complex. Continuing with our bidisperse example, a given parent phase will start to phase separate at the cloud point as T is lowered. For lower temperatures, two phases will coexist in finite amounts; at each given T, the densities ρ_1 and ρ_2 in these phases can be found from the ends of the unique tie line (in the ρ_1–ρ_2 plane) that passes through the parent. Neither of the coexisting phases will therefore be on the dilution line (see figure 2), and both will contain different fractions of particles of the two species; only the overall composition across the two phases will be maintained. Plotting the temperature against the total density of the two phases would generate two 'coexistence' curves which begin on the cloud and shadow curve, respectively (see figure 3). Each parent on the dilution line will generate its own set of coexistence curves, all beginning at different points on the cloud and shadow curves.

So far I have only discussed situations where at most two phases coexist once phases separation occurs. In a polydisperse system, this need not be the case, of course; as discussed above, there is no *a priori* limit on the number of coexisting phases. To see the qualitative effect of this on the representations of phase behaviour described above, let us return to the bidisperse case, but now with a different phase diagram, shown in figure 4. This phase diagram topology could occur in, for example, a binary liquid whose constituent particles 'dislike' each other; in addition to the usual gas–liquid phase coexistence one can then also have demixing into two liquids containing predominantly one of the particle species, and three-phase coexistence between a gas and two such demixed liquids. A dilute cloud phase may then begin to phase separate by splitting off either one of these demixed liquids, depending on the relative positions of the dilution line and the three-phase triangle (see figure 4). As temperature is varied, a corner of the three-phase triangle may move through the dilution line. At the temperature where this

happens, the cloud phase is at a triple point, and separates off infinitesimal amounts of *two different* shadow phases; as T is increased or decreased through the triple point, the properties of the shadow phase therefore 'switch' discontinuously. This implies that the shadow curve will exhibit a jump discontinuity, while the cloud curve remains connected as it must but will have a kink where the shadow curve jumps (see figure 4). The coexistence curves also become more complex: a parent may initially separate into two phases, but then demix into three (or more, in the fully polydisperse case) as T is lowered further; at the points where new phases appear, the coexistence curves acquire new branches. For even lower temperatures, the number of phases may increase yet further, or decrease again. It is in fact an entirely open problem to predict from the form of the free energy the maximum number of phases into which a given polydisperse parent phase will separate.

One final new feature in the phase behaviour of polydisperse systems is the possibility of encountering critical points of arbitrary order. Such critical points are specified by a density distribution $\rho(\sigma)$ and a temperature T; their defining property is that, at those parameters, a single phase separates into n infinitesimally different phases (on lowering T, for example). Thus $n = 2$ is an ordinary critical point, $n = 3$ a tricritical point, and so on [22, 23]. Since there is no limit on the number of coexisting phases, it is intuitively clear that there is also no upper limit on the order of critical points that can occur in polydisperse systems. We will see a concrete example of this below, for a simple model of a random copolymer blend.

2.3. Formulating the general phase equilibrium problem

The statistical mechanics of polydisperse systems is also known as 'continuous thermodynamics' (see e.g. [24]). It is often useful to separate off the ideal part of the free energy (density) explicitly by writing (with $k_B = 1$)

$$f([\rho(\sigma)]) = T \int \mathrm{d}\sigma\, \rho(\sigma)[\ln \rho(\sigma) - 1] + \tilde{f}([\rho(\sigma)]). \tag{3}$$

This defines the excess free energy $\tilde{f}$; both f and $\tilde{f}$ are functionals of the density distribution $\rho(\sigma)$ (and also functions of the externally fixed temperature, which I will not write explicitly). The ideal part is the free energy of an ideal polydisperse gas; it can be derived as the limiting form (up to an irrelevant—infinite—constant term [20]) of the free energy of an ideal mixture of M species, which is $T \sum_i \rho_i[\ln \rho_i - 1]$. Here the ρ_i are again the number densities inside M 'bins' into which the range of σ has been partitioned, and the number of bins is taken to infinity *after* the thermodynamic limit has been performed. In an alternative derivation of the polydisperse limit, one can assume from the start that all particles are genuinely different, with σ sampled randomly from the normalized density distribution, so that the number of distinct 'species' is always N and is taken to infinity together with the system size. The two procedures give equivalent results [25]; an elegant derivation of the ideal part of the free energy within the second approach was given by Warren [26]. Note that the first limit is physically more plausible for many homopolymer systems (where there may only be thousands or millions of species, with many particles of each) whereas the second limit is more natural for colloidal materials (and also some random copolymers) in which no two particles present are exactly alike, even in a sample of macroscopic size.

From the free energy (3), the chemical potentials follow by (functional) differentiation as

$$\mu(\sigma) = \frac{\delta f}{\delta \rho(\sigma)} = T \ln \rho(\sigma) + \tilde{\mu}(\sigma) \qquad \tilde{\mu}(\sigma) = \frac{\delta \tilde{f}}{\delta \rho(\sigma)}. \tag{4}$$

The pressure is, by analogy with (1),

$$\Pi = -f + \int \mathrm{d}\sigma\, \mu(\sigma)\rho(\sigma) = T\rho_0 - \tilde{f} + \int \mathrm{d}\sigma\, \tilde{\mu}(\sigma)\rho(\sigma) \tag{5}$$

where

$$\rho_0 = \int \mathrm{d}\sigma\, \rho(\sigma) \tag{6}$$

is the total number density of particles. Though not written explicitly, both $\mu(\sigma)$ and Π are functionals of $\rho(\sigma)$, and ordinary functions of T. Note also that, in order avoid 'dimensional crimes' in the logarithms in f and $\mu(\sigma)$, equations (3), (4), one should really divide the argument $\rho(\sigma)$ by a quantity with the same dimensions, with e.g. making the replacement $\rho(\sigma) \to v_0\sigma_0\rho(\sigma)$ (where v_0 and σ_0 are chosen unit values of volume and of σ) or $\rho(\sigma) \to \rho(\sigma)/R(\sigma)$ where $R(\sigma)$ is a fixed density distribution. As can be seen from (4), however, any such replacement would only add a $[\rho(\sigma)]$-independent term to the chemical potentials and so would not affect the predicted phase equilibria; we can therefore proceed without it. (In the moment free energy method to be described below, however, the fact that an arbitrary $R(\sigma)$ can be chosen to non-dimensionalize $\rho(\sigma)$ will be of crucial importance.)

Assume now that a given parent phase with density distribution $\rho^{(0)}(\sigma)$ separates into P phases, labelled as before by $\alpha = 1, \ldots, P$ and with density distributions $\rho^{(\alpha)}(\sigma)$. Then the chemical potentials $\mu(\sigma)$ and the pressure Π need to be equal in all phases, and the total number of particles of each species σ must be conserved, implying that

$$\sum_\alpha v^{(\alpha)}\rho^{(\alpha)}(\sigma) = \rho^{(0)}(\sigma) \tag{7}$$

where, as in (2), $v^{(\alpha)}$ is the fraction of the system volume occupied by phase α.

From (4), it follows that $\rho^{(\alpha)}(\sigma) = \exp[\beta\mu(\sigma)]\exp[-\beta\tilde{\mu}^{(\alpha)}(\sigma)]$, where $\beta = 1/T$ and $\tilde{\mu}^{(\alpha)}(\sigma)$ is the excess chemical potential of species σ in phase α. Inserting into the particle conservation law (7), one can eliminate $\exp[\beta\mu(\sigma)]$ and write the density distributions in the coexisting phases as

$$\rho^{(\alpha)}(\sigma) = \rho^{(0)}(\sigma)\frac{\exp[-\beta\tilde{\mu}^{(\alpha)}(\sigma)]}{\sum_\gamma v^{(\gamma)}\exp[-\beta\tilde{\mu}^{(\gamma)}(\sigma)]}. \tag{8}$$

The P unknown fractional phase volumes can then in principle be determined from the equality of the pressure in all phases and from the identity $\sum_\alpha v^{(\alpha)} = 1$. However, in (8) we have achieved no more than a formal solution of the problem, since the excess chemical potentials $\tilde{\mu}^{(\alpha)}(\sigma)$ are still functionals of the unknown density distributions $\rho^{(\alpha)}(\sigma)$ (so, if these functionals can be written as integrals, equation (8) corresponds in effect to P coupled non-linear integral equations [27]). Even if a valid solution for a phase split into P phases could be determined numerically, one would still need to verify that it is thermodynamically stable, i.e. that it gives the lowest possible total free energy; this problem is exacerbated in a polydisperse system by the potentially unlimited number of coexisting phases. In principle, the criterion for stability is that no part of the free energy surface 'pokes through' below the calculated tangent plane; equivalently, an appropriately defined tangent plane distance [28] needs to be everywhere non-negative. Like f, however, the tangent plane distance is a *functional* of $\rho(\sigma)$, so a numerical search over all its values is clearly impossible.

If one restricts oneself to finding not full phase splits, but just the spinodal at which a given parent phase first becomes locally unstable, one still faces a non-trivial task. A local instability corresponds to a 'direction' $\delta\rho(\sigma)$ in density distribution space along which the curvature of the free energy 'surface' vanishes (see e.g. [23, 29]), such that

$$\int \mathrm{d}\sigma\, \frac{\delta^2 f}{\delta\rho(\sigma)\,\delta\rho(\sigma')}\,\delta\rho(\sigma') = 0 \tag{9}$$

where the derivative is evaluated at the parent $\rho^{(0)}(\sigma)$. (I will not study here the subtle question of how, beyond the approximate mean-field-type models discussed below, free energies can actually be defined in spinodal and unstable regions; see e.g. [30].) The spinodal temperature T can thus in principle be found as the temperature where, coming from a region of stability, this equation first has a non-zero solution $\delta\rho(\sigma)$.

2.4. Truncatable free energies

As explained above, predicting phase equilibria for a polydisperse system with a completely generic free energy functional is next to impossible. However, an important insight—later rediscovered by a number of authors, and summarized in the most general terms probably by Hendriks [31–33]—came from the seminal work of Gualtieri *et al* [27]: significant progress can be made for (model) systems with so-called 'truncatable' free energies [23]. These are characterized by an *excess* contribution $\tilde{f} = \tilde{f}(\{\rho_i\})$ that depends only on a finite number, K (say), of generalized *moment densities*

$$\rho_i = \int \mathrm{d}\sigma\, w_i(\sigma)\rho(\sigma) \tag{10}$$

of the density distribution $\rho(\sigma)$; for power-law weight functions $w_i(\sigma) = \sigma^i$, the ρ_i are conventional moments. The term 'truncatable' emphasizes that the number of moment densities appearing in the excess free energy of truncatable models is finite, while for a non-truncatable model the excess free energy depends on all details of $\rho(\sigma)$, corresponding to an *infinite* number of moment densities. The class of polydisperse systems whose (at least approximate) free energies are truncatable is surprisingly large; a number of examples are given in section 4 below. I will normally assume that the total particle density ρ_0, corresponding to the weight function $w_0(\sigma) = 1$, is included in the set of moment densities.

For a truncatable system, the excess chemical potentials can be written as

$$\tilde{\mu}(\sigma) = \frac{\delta\tilde{f}}{\delta\rho(\sigma)} = \sum_i w_i(\sigma)\tilde{\mu}_i \tag{11}$$

where

$$\tilde{\mu}_i = \frac{\partial\tilde{f}}{\partial\rho_i} \tag{12}$$

are excess moment chemical potentials. The density distributions (8) in the different phases can thus be written as

$$\rho^{(\alpha)}(\sigma) = \rho^{(0)}(\sigma)\frac{\exp\left[\sum_i \lambda_i^{(\alpha)} w_i(\sigma)\right]}{\sum_\gamma v^{(\gamma)} \exp\left[\sum_i \lambda_i^{(\gamma)} w_i(\sigma)\right]} \tag{13}$$

where the $\lambda_i^{(\alpha)}$ must obey

$$\lambda_i^{(\alpha)} = -\beta\tilde{\mu}_i^{(\alpha)} + c_i. \tag{14}$$

The constants c_i (common to all P phases, with one for each moment density) occur here since a common shift of all the $\lambda_i^{(\alpha)}$ for any fixed i leaves the density distributions (13) unchanged. One can fix this indeterminacy by, for example, setting all $c_i = 0$, or fixing all the $\lambda_i^{(\alpha)}$ in one of the phases to be zero. Either way, we have with (14) a set of $P \times K$ non-linear equations for the $P \times K$ parameters $\lambda_i^{(\alpha)}$. At fixed values of the $v^{(\alpha)}$, these equations are closed: from the $\lambda_i^{(\alpha)}$ one can find, via (13) and (10), the $\rho_i^{(\alpha)}$ and hence the $\tilde{\mu}_i^{(\alpha)}$ (which, for a truncatable model, are functions of the moment densities in the respective phase only). The remaining

P parameters $v^{(\alpha)}$ are found again from $\sum_\alpha v^{(\alpha)} = 1$ and from the equality of the pressure (using (5))

$$\Pi = T\rho_0 - \tilde{f} + \sum_i \tilde{\mu}_i \rho_i \tag{15}$$

in all phases. So the calculation of a phase split of a given parent into P phases requires, for a truncatable model, the solution of $P(K+1)$ non-linear coupled equations for the same number of variables. Starting from a suitable initial guess, such a solution can, in principle, be found by a standard algorithm such as the Newton–Raphson one [34]. (Generating an initial point from which such an algorithm will converge, however, is a non-trivial problem, especially when more than two phases coexist and/or many moment densities are involved.) There is also, for truncatable systems, a well-defined way of checking whether a calculated phase split is thermodynamically stable: rather than over the infinite-dimensional space of density distributions $\rho(\sigma)$, the tangent plane distance now needs to be searched only over a K-dimensional space, which is possible numerically using Monte Carlo methods [23].

If one is interested only in finding the cloud point for a given parent distribution (rather than phase splits inside the coexistence region), the problem becomes rather simpler. At the cloud point there is coexistence between the parent $\rho^{(0)}(\sigma)$, which still occupies all of the system volume ($v^{(0)} = 1$), and P shadow phases $\rho^{(\alpha)}(\sigma)$ which are present in vanishingly small amounts ($v^{(\alpha)} = 0$ for $\alpha = 1, \ldots, P$). In the generic situation there is only a single shadow ($P = 1$) but higher values of P can occur, e.g. $P = 2$ at a triple point (where, as discussed above, a cloud phase coexists with two shadows). Using our freedom to choose the λ_i in one phase to fix $\lambda_i^{(0)} = 0$, we then have from (13) that the shadow phase density distributions are given by

$$\rho^{(\alpha)}(\sigma) = \rho^{(0)}(\sigma) \exp\left[\sum_i \lambda_i^{(\alpha)} w_i(\sigma)\right] \tag{16}$$

and that their $\lambda_i^{(\alpha)}$ must obey

$$\lambda_i^{(\alpha)} = -\beta\tilde{\mu}_i^{(\alpha)} + \beta\tilde{\mu}_i^{(0)}. \tag{17}$$

For an ordinary cloud point ($P = 1$) there is then only one additional equation, the equality of pressure between cloud (parent) and shadow, and this fixes the cloud point temperature. (For larger P the pressure equalities give $P - 1$ additional conditions on the parent distribution $\rho^{(0)}(\sigma)$; for $P = 2$, for example, this condition determines at what parent density the triple point occurs.)

Even more drastic simplifications occur, finally, in the spinodal and critical point criteria for truncatable systems. In particular, it has been shown that the spinodal criterion involves only the moment densities ρ_i of the parent phase, as well as its 'second-order moment densities' $\rho_{ij} = \int \mathrm{d}\sigma\, w_i(\sigma) w_j(\sigma) \rho^{(0)}(\sigma)$ [23, 29, 32, 33, 35–38]. This simplification is particularly useful if the moment densities are ordinary moments, i.e. if the weight functions are simple powers $w_i(\sigma) = \sigma^i$ ($i = 0, \ldots, K-1$); then the spinodal criterion only involves the parent moments up to $\mathcal{O}(\sigma^{2K-2})$. The condition for critical points depends additionally on the third-order moment densities ρ_{ijk} defined in the obvious way [23,36,39], and generally one can show that the criterion for an n-critical point will involve up to $(2n-1)$th-order moment densities.

3. Methods

3.1. Direct numerical solution

For simple truncatable models involving only $K = 1$ or 2 moment densities, a direct numerical solution of the phase equilibrium equations as given above is often possible—

see e.g. [24, 33, 40–44]; I will review the results of some of these calculations below, in the context of the various models that have been studied (section 4). Apart from general-purpose tools for solving non-linear coupled equations (see e.g. [34]), a number of more specialized numerical techniques have been developed for this purpose. Popular in particular in the chemical engineering literature is the method of 'successive substitution'. This is based on an iteration loop where at each iteration one first holds the excess chemical potentials $\tilde{\mu}^{(\alpha)}(\sigma)$ (or, in a truncatable system, the $\lambda_i^{(\alpha)}$) fixed and finds the fractional phase volumes from the conditions of pressure equality; this then determines the density distributions, from which one can re-calculate the excess chemical potentials and return to the beginning of the loop [45,46]. (Under conditions of constant pressure rather than constant volume as considered here, the first part of the iteration can be formulated as a minimization problem over the $v^{(\alpha)}$ [47].) Various accelerations and variants of this method have been proposed [28, 48–50]; a serious disadvantage is, however, that the iteration can become unstable and fail to converge [51]. For the task of tracing out cloud and shadow curves (rather than following the phase behaviour of a given parent phase as external control parameters such as temperature are varied), specialized techniques have also been developed—see e.g. [52]—with refinements for the numerically often difficult regions around critical points [53].

3.2. Binning and pseudo-components; method of moments

For an approximate solution of the polydisperse phase equilibrium problem, the most straightforward method is to 'bin' the full density distribution $\rho(\sigma)$ into a number of discrete 'pseudo-components', whose densities are given by the density of particles within the respective σ-ranges. This then formally reduces the problem to that of a finite mixture. The pseudo-components can be spaced evenly across the σ-range, or chosen according to other *ad hoc* prescriptions. For simple functional forms of the parent distribution $\rho^{(0)}(\sigma)$ it has been suggested, for example, that one could locate the pseudo-components at those σ-values which would be used in a Gaussian quadrature with $\rho^{(0)}(\sigma)$ as the weight function [54–56]. Some slight improvement in accuracy is also possible by keeping track (to linear order) of variations in the parent distribution across each bin [57]. Whatever particular implementation is chosen, however, it is clear that binning introduces uncontrolled systematic errors and also becomes numerically unwieldy for large numbers of pseudo-components.

A somewhat more systematic approach to allocating pseudo-components is the method of 'r-equivalent distributions' [35, 58]. Here the parent distribution $\rho^{(0)}(\sigma)$ is replaced by a mixture of a finite number of species whose σ-values and densities are chosen to match exactly the first r moments of $\rho^{(0)}(\sigma)$; this approach has also been used in the determination of single-phase properties such as correlation functions [56]. If one is studying a truncatable model (with power-law weight functions), then since the conditions for spinodals and critical points depend on only a finite number of moments of $\rho^{(0)}(\sigma)$, these points will be found exactly if r is chosen large enough. The results for actual phase splits, however, including the onset of phase coexistence (cloud points and shadows), will be only approximate.

An alternative (but still uncontrolled) approximation is the 'method of moments'. This retains the continuous range of σ but fixes a parametric form for the density distributions in all phases (e.g. Gaussian or Schulz; the Schulz distribution has the form $\rho(\sigma) \sim \sigma^{\alpha} \mathrm{e}^{-\sigma/\sigma_0}$). The free parameters specifying these distributions are then found by solving the phase equilibrium equations approximately, requiring particle conservation only for certain moments of the parent density distribution $\rho^{(0)}(\sigma)$ rather than all its details [54,59–61]. A similar idea was used in [62] to reduce the problem of finding cloud points and shadows to a set of (approximate) non-linear equations in a finite number of variables.

3.3. Perturbative methods for nearly monodisperse systems

For systems which are nearly monodisperse, one can pursue systematic perturbation expansions around a monodisperse reference system. These can never hope to capture qualitative polydispersity-induced changes in the phase diagram, such as the appearance of new phases. However, they can still give some important insights into the effects of 'weak' polydispersity, predicting for example the trends in the fractionation across coexisting phases, or whether polydispersity tends to narrow or widen coexistence regions in the phase diagram.

The first of such perturbation theories was probably that of Gualtieri *et al* [27]. They assumed that the parent density distributions consisted of a dominant monodisperse part ($\rho^{(0)}(\sigma) \sim \delta(\sigma - \sigma_0)$), with a small amount of polydisperse material added. The overall fraction of polydisperse material was used as the expansion parameter and therefore constrained to be small, but there was no restriction on the width (σ-range) of the polydisperse component. A number of other authors took a complementary approach, assuming that the overall range of σ-values in the parent is narrow and expanding perturbatively in this small width, often assuming a simple functional form for the parent distribution such as a Gaussian [62–64].

More recently, Evans [65–67] has re-examined the perturbative approach and shown, in particular, that the actual shape of the parent distribution is irrelevant (it can even consist of a number of closely spaced δ-peaks, corresponding to a discrete mixture of very similar species) as long as it is sufficiently narrow. In Evans' approach, it is useful to factor the overall density out of the density distribution, decomposing it as $\rho(\sigma) = \rho_0 n(\sigma)$ where $n(\sigma)$ is the normalized σ-distribution ($\int \mathrm{d}\sigma\, n(\sigma) = 1$). If the normalized parent distribution $n^{(0)}(\sigma)$ is sufficiently narrow, with mean $\bar{\sigma}$, then $\epsilon = (\sigma - \bar{\sigma})/\bar{\sigma}$ will be small in all coexisting phases; it is then convenient to switch from σ to ϵ as the polydisperse attribute. Evans now assumes that the excess free energy (density) of an arbitrary phase with density distribution $\rho(\epsilon) = \rho_0 n(\epsilon)$ can be expanded systematically as

$$\beta \tilde{f} = \tilde{f}_{\mathrm{m}}(\rho_0) + \langle\epsilon\rangle\, A(\rho_0) + \langle\epsilon^2\rangle B(\rho_0) + \langle\epsilon\rangle^2\, C(\rho_0) + \mathcal{O}(\epsilon^3) \tag{18}$$

where $\langle\epsilon\rangle = \int \mathrm{d}\epsilon\, \epsilon n(\epsilon)$ and similarly for $\langle\epsilon^2\rangle$, and $\tilde{f}_{\mathrm{m}}(\rho_0)$ is the excess free energy of a monodisperse reference system (with $\epsilon = 0$, i.e. $\sigma = \bar{\sigma}$ for all particles). The coefficients A, B, and C are unspecified functions of the overall density ρ_0. From this very generic form a number of elegant results follow. For example, for the normalized ϵ-distribution in a phase α coexisting with one or more other phases, one finds

$$n^{(\alpha)}(\epsilon) = n^{(0)}(\epsilon)\left[1 - \epsilon\left(\frac{A^{(\alpha)}}{\rho_0^{(\alpha)}} - \frac{1}{\rho_0^{(0)}}\sum_{\beta} v^{(\beta)} A^{(\beta)}\right)\right] + \mathcal{O}(\epsilon^2) \tag{19}$$

where the coefficients $A^{(\alpha)} \equiv A(\rho_0^{(\alpha)})$ can be evaluated at the densities of the coexisting phases in either the monodisperse reference system or the actual polydisperse system, the difference contributing only to the neglected $\mathcal{O}(\epsilon^2)$ terms. Taking the first moment of (19), one has for the difference of $\langle\epsilon\rangle$ in two coexisting phases

$$\langle\epsilon\rangle^{(\alpha)} - \langle\epsilon\rangle^{(\beta)} = -s^2\left(\frac{A^{(\alpha)}}{\rho_0^{(\alpha)}} - \frac{A^{(\beta)}}{\rho_0^{(\beta)}}\right) \tag{20}$$

where s, defined through

$$s^2 = \int \mathrm{d}\epsilon\, \epsilon^2 n^{(0)}(\epsilon) = \int \mathrm{d}\sigma\, \left(\frac{\sigma - \bar{\sigma}}{\bar{\sigma}}\right)^2 n^{(0)}(\sigma) \tag{21}$$

is the standard deviation of the parent distribution normalized by its mean, often simply called the polydispersity. The 'universal fractionation law' [65,66,68] of equation (20) states that the

difference in the mean of the particle sizes (or whatever polydisperse attribute ϵ measures) in coexisting phases is directly proportional to the *variance* of the parent distribution. The result is valid for arbitrary (narrow) parent distributions, including non-smooth ones. Results for the polydispersity-induced shifts of phase boundaries relative to the monodisperse reference system can also be derived, and are again found to be proportional to the variance s^2 of the parent distribution (rather than, as one might have naively expected, to its standard deviation s). In the region near critical points, the perturbative expansion for the phase boundaries breaks down, since polydispersity generally shifts the location of the critical point to a different temperature; at the critical point of the monodisperse reference system, a polydisperse system will thus show either non-critical phase coexistence (between non-identical phases), or no phase separation at all. Nevertheless, the approach is useful, particularly if one is interested in questions such as whether polydispersity will lead to a widening or a narrowing of the coexistence gap in any given system. It also generalizes straightforwardly to the case of several polydisperse attributes, where ϵ becomes a vector-valued variable [67].

3.4. Moment free energy method

As pointed out above, even for truncatable models the numerical solution of the phase equilibrium conditions can be an extremely difficult numerical problem. Furthermore, the non-linear phase equilibrium equations permit no simple geometrical interpretation or qualitative insight akin to the familiar rules for constructing phase diagrams from the free energy surface of a finite mixture. To address these two disadvantages, one can construct a so-called 'moment free energy' [23, 26, 69]. This takes the above insights for truncatable systems further, by showing that a simplification similar to that for the phase equilibrium conditions exists also on the level of the free energy itself.

There are (at least) two approaches to constructing the moment free energy; I describe here the so-called projection method [69]. The starting point is the decomposition (3) for the free energy of truncatable systems

$$f = T \int \mathrm{d}\sigma\, \rho(\sigma) \left[\ln \frac{\rho(\sigma)}{R(\sigma)} - 1 \right] + \tilde{f}(\{\rho_i\}). \tag{22}$$

In the first (ideal) term of (22), a dimensional factor $R(\sigma)$ has been included inside the logarithm; while this has no effect on the exact thermodynamics (see above), it will play a central role below.

To motivate the construction of the moment free energy, one can argue that the most important moment densities to treat correctly in the calculation of phase equilibria are those that actually appear in the excess free energy $\tilde{f}(\{\rho_i\})$. Accordingly one divides the infinite-dimensional space of density distributions into two complementary subspaces: a 'moment subspace', which contains all the degrees of freedom of $\rho(\sigma)$ that contribute to the moment densities ρ_i, and a 'transverse subspace' which contains all remaining degrees of freedom (those that can be varied without affecting the chosen moment densities ρ_i). Physically, it is reasonable to expect that these 'leftover' degrees of freedom play a subsidiary role in the phase equilibria of the system, a view that can be justified *a posteriori*. Accordingly, one now allows violations of the lever rule, so long as these occur *solely in the transverse space*. This means that the phase splits calculated using this approach obey particle conservation for the moment densities, but are allowed to violate it in other details of the density distribution $\rho(\sigma)$. These 'transverse' degrees of freedom are instead chosen so as to minimize the free energy: they are treated as 'annealed'. Because the excess free energy depends (for a truncatable system) only on the set of moment densities, one therefore has to minimize the ideal part of the free energy

over all distributions $\rho(\sigma)$ with fixed moment densities ρ_i. This yields

$$\rho(\sigma) = R(\sigma) \exp\left[\sum_i \lambda_i w_i(\sigma) \right] \tag{23}$$

where the Lagrange multipliers λ_i are chosen to give the desired moment densities:

$$\rho_i = \int \mathrm{d}\sigma \; w_i(\sigma) R(\sigma) \exp\left[\sum_j \lambda_j w_j(\sigma) \right]. \tag{24}$$

The corresponding minimum value of f then defines the *moment free energy* as a function of the moment densities ρ_i:

$$f_{\mathrm{mom}}(\{\rho_i\}) = T\left(\sum_i \lambda_i \rho_i - \rho_0 \right) + \tilde{f}(\{\rho_i\}). \tag{25}$$

Since the Lagrange multipliers are (at least implicitly) functions of the moment densities, the moment free energy depends only on the set of moment densities. These can now be viewed as densities of 'quasi-species' of particles, allowing for example the calculation of 'moment chemical potentials' [23]

$$\mu_i = \frac{\partial f_{\mathrm{mom}}}{\partial \rho_i} = T\lambda_i + \frac{\partial \tilde{f}}{\partial \rho_i} = T\lambda_i + \tilde{\mu}_i \tag{26}$$

and the corresponding pressure

$$\Pi = \sum_i \mu_i \rho_i - f_{\mathrm{mom}} = T\rho_0 + \sum_i \tilde{\mu}_i \rho_i - \tilde{f} \tag{27}$$

(which for truncatable systems is identical to the exact expression (15)). A finite-dimensional phase diagram can thus be constructed from f_{mom} according to the usual tangency plane rules, ignoring the underlying polydisperse nature of the system. Obviously, though, the results now depend on $R(\sigma)$ which is formally a 'prior distribution' for the free energy minimization. *Geometrically*, its effect is to tilt the free energy surface before it is 'projected' onto the moment subspace; this point of view is explained in detail in [23]. To understand the influence of $R(\sigma)$ *physically*, one notes that the moment free energy is simply the free energy of phases in which the density distributions $\rho(\sigma)$ are of the form (23). The prior $R(\sigma)$ determines which distributions lie within this 'family', and it is the properties of phases with these distributions that the moment free energy represents. To ensure that the parent phase is contained in the family, one chooses its density distribution as the prior, $R(\sigma) = \rho^{(0)}(\sigma)$; the moment free energy procedure will then be *exactly valid* whenever the density distributions *actually arising* in the various coexisting phases of the system under study *are members of the corresponding family*

$$\rho(\sigma) = \rho^{(0)}(\sigma) \exp\left[\sum_i \lambda_i w_i(\sigma) \right]. \tag{28}$$

This condition holds whenever all but one of a set of coexisting phases are of infinitesimal volume compared to the majority phase, as can be seen explicitly from (16). Accordingly, the moment free energy yields *exact* cloud point and shadow curves. (And the exact conditions (14) are seen, with the help of (26), to express precisely the requirement of equal moment chemical potentials in all phases.) Similarly, one can show that spinodals and critical points of any order are found exactly [23]. For coexistences involving finite amounts of different phases the moment free energy only gives approximate results, since different density distributions from the family (28), corresponding to two (or more) phases arising from the same parent $\rho^{(0)}(\sigma)$, do not in general add to recover the parent distribution itself. Moreover, according to

Gibbs' phase rule, a moment free energy depending on K moment densities will not normally predict more than $K + 1$ coexisting phases, whereas we know that a polydisperse system can in principle separate into an arbitrary number of phases. Both of these shortcomings can be overcome by including extra moment densities within the moment free energy; this does not affect any of the exactness statements above but systematically increases the accuracy of any calculated phase splits [23]. This idea can be further refined by choosing the weight functions of the extra moments adaptively, which allows the properties of the coexisting phases to be predicted with in principle arbitrary accuracy [70].

The moment free energy method (or moment method for short) thus restores to the problem of polydisperse phase equilibria much of the physical and geometrical insight available from the thermodynamics of finite mixtures. It also leads to computationally efficient procedures; in particular, its numerical implementation can handle coexistence of more than two phases with relative ease compared to previous approaches [28,32,47,49,52,54,55,58,59,62,71,72].

4. Applications to (model) systems

4.1. Polymers I: Flory–Huggins theory for homopolymers

Flory–Huggins theory [73] is a simple but remarkably successful approximate theory describing the thermodynamics of polymer solutions and blends. It was derived in the 1940s [6–8] and extended very early on to include polydispersity in the lengths of the polymer chains. For clarity I will use L here rather than σ for the polydisperse attribute, so $\rho(L)\,\mathrm{d}L$ will be the number density of polymers with lengths in the range $[L, L+\mathrm{d}L]$. The excess free energy of polydisperse Flory–Huggins theory for homopolymers (which contain only one type of monomer) is then

$$\tilde{f} = (1-\rho_1)\ln(1-\rho_1) + \chi\rho_1(1-\rho_1) \tag{29}$$

where $w_1(L) = L$ and I have set $k_\mathrm{B}T = 1$. I have also chosen the volume of a solvent molecule as the unit volume, and assumed for simplicity that this is equal to the volume of a monomer (or polymer 'segment'); ρ_1 is then simply the volume fraction of polymer. The first term in $\tilde{f}$ is minus the entropy of the solvent and always leads to an increase in free energy when phase separation occurs. The second term, on the other hand, reflects the interactions of the monomers with each other and with the solvent, with χ measuring the effective monomer–monomer attraction in units of $k_\mathrm{B}T$. When (as T is lowered) χ becomes sufficiently large, this attraction causes a phase separation into a polymer-rich and a polymer-poor phase; in the monodisperse case, this is the only phase separation that occurs. Tompa [74, 75], however, realized that already bidisperse polymer solutions can exhibit three-phase coexistence as soon as the ratio of the two different chain lengths is larger than around ten; this then produces a kink in the cloud curve and a jump in the shadow curve as discussed in section 2. Solc [13] realized that, in fact, rather intricate phase diagram topologies can occur: as sketched in figure 5, the occurrence of the three-phase coexistence can end up 'removing' the critical point from the cloud curve, by shifting it onto a metastable or unstable branch of the cloud curve where it is no longer accessible.

Of course, three-phase coexistence will be observed not only for the parent density at which the cloud curve has its kink (i.e., directly at the triple point), but also for a range of temperatures and densities around this point. Not unexpectedly, the maximum temperature interval over which three-phase coexistence can be observed (for an appropriately chosen composition of the system) becomes wider as the lengths of the two polymer species becomes more disparate; conversely, it can shrink to zero as they become comparable. Where this

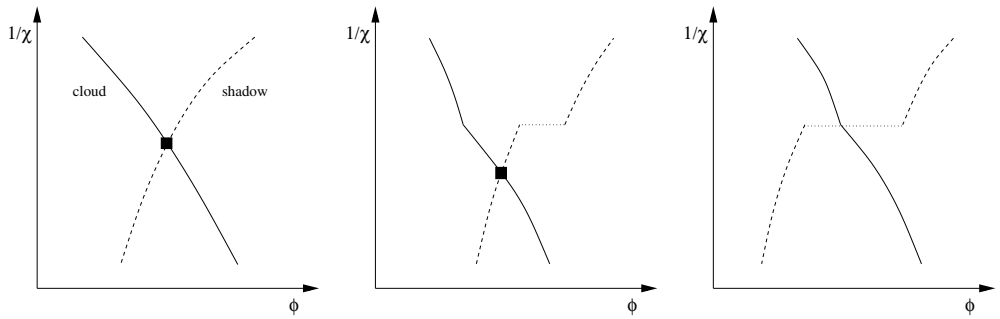

Figure 5. Qualitative cloud and shadow curves for homopolymers with chain length polydispersity. Only the region around the critical point (which is marked by a rectangle) is shown; cloud curves are solid and shadow curves dashed. As is conventional, the polymer volume fraction (rather than number density) is used on the x-axis to specify the overall dilution of the system; on the y-axis, since χ is measured in units of k_BT, $1/\chi$ is essentially a dimensionless temperature. Left: the conventional phase diagram topology, which is found for monodisperse or weakly polydisperse systems. Middle: as the length polydispersity increases, a triple point can occur where the shadow curve has a jump discontinuity. Right: for even more pronounced polydispersity, the triple point may prevent the crossing of cloud and shadow curves, thus making the critical point inaccessible.

happens, one gets a tricritical point, as was first realized by Solc *et al* [76] and later confirmed experimentally [53,77–80]. For mixtures of more than two polymer species with appropriately tuned length distributions, higher-order critical points can also occur [81]. Finally, more complicated phase separation sequences including even re-entrant features are possible; for a specific solution of a mixture of three different polymer species, for example, a sequence of one → three → two → three phases was observed on lowering the temperature [82].

All the results above were for mixtures of a small number of distinct polymer species whose chain lengths were assumed to be sharply defined. For truly polydisperse systems, the first numerical calculations of phase equilibria were probably those of Koningsveld and Staverman [10–12,21], with an emphasis on using fractionation effects to generate phases with a narrow distribution of chain lengths. Solc [13,83] realized later that three-phase coexistence is quite generic in distributions of chain lengths which have 'fat tails' (which means, in this context, that they decay more slowly than exponentially with L for large lengths). In such systems he predicted the critical point to be always 'hidden', corresponding to the most extreme polydisperse case sketched in figure 5, and this was later confirmed experimentally [84].

In fact, 'fat-tailed' parent distributions give rise to quite subtle behaviour, in particular for the cloud and shadow curves. To explain how this arises, I will paraphrase Solc's arguments [13, 83] here. Flory–Huggins theory for homopolymers gives, as can be seen from (29), a truncatable free energy with a single moment density ρ_1, with excess moment chemical potential

$$\tilde{\mu}_1 = -1 - \ln(1-\rho_1) + \chi(1-2\rho_1) \tag{30}$$

and osmotic pressure

$$\Pi = \rho_0 + \rho_1\tilde{\mu}_1 - \tilde{f} = \rho_0 - \rho_1 - \ln(1-\rho_1) - \chi\rho_1^2. \tag{31}$$

The solvent entropy leads to a positive contribution $-\rho_1 - \ln(1-\rho_1)$ to Π, acting against increases in polymer volume fraction ρ_1, while the monomer–monomer attraction gives the negative term $-\chi\rho_1^2$ favouring large values (but <1) of ρ_1.

Consider now the shadow phase coexisting with the parent at the cloud point. From (17), its density distribution has the form $\rho^{(1)}(L) = \rho^{(0)}(L)\exp(\lambda_1^{(1)}L)$. If we drop the superscript

on the shadow phase properties and use the abbreviation $\lambda \equiv \lambda_1^{(1)}$ this is written simply as

$$\rho(L) = \rho^{(0)}(L) \exp(\lambda L) \tag{32}$$

and the condition on λ—sometimes called the 'separation parameter' in the polymer literature—is, from (17),

$$\lambda_i = \beta\tilde{\mu}_1^{(0)} - \beta\tilde{\mu}_1. \tag{33}$$

The value of χ at the cloud point, finally, can be found from the pressure equality $\Pi = \Pi^{(0)}$.

Equation (32) shows clearly why a slower-than-exponential decay of the parent distribution for large L will lead to unusual effects: a positive value of λ causes all moments of the shadow phase distribution $\rho(\sigma)$ to diverge. In fact, to get well-defined results one needs to impose—as is physically reasonable—a cut-off on the parent distribution at some large length $L_{\max}$, and then consider the limit[1] of large $L_{\max}$. Cloud–shadow pairs with negative λ—corresponding to a dense cloud phase and a more dilute shadow—will be only very weakly affected by the value of $L_{\max}$, since no diverging integrals occur even for $L_{\max} \to \infty$. For positive λ, on the other hand, one needs to consider carefully the dependence of λ on $L_{\max}$. A first possibility is that λ has a non-zero limit for $L_{\max} \to \infty$. But then the integral for the shadow's polymer volume fraction $\rho_1 = \int \mathrm{d}L\, L\rho^{(0)}(L) \exp(\lambda L)$ will diverge unless the parent (cloud phase) density $\rho_0^{(0)}$ converges to zero such as to give a limiting $\rho_1 < 1$. The polymer density ρ_0 of the shadow will then also converge to zero, since the shadow phase is dominated by the longest polymer chains and thus $\rho_0 \sim \rho_1/L_{\max} \to 0$. From (31), the osmotic pressure of the shadow phase is then

$$\Pi = -\rho_1 - \ln(1-\rho_1) - \chi\rho_1^2. \tag{34}$$

The parent, on the other hand, has $\Pi^{(0)} = 0$ because of its vanishing polymer density $\rho_0^{(0)}$ (and hence polymer volume fraction $\rho_1^{(0)}$). The pressure equality thus gives $\Pi = 0$, or

$$\chi = \frac{-\rho_1 - \ln(1-\rho_1)}{\rho_1^2}. \tag{35}$$

Remarkably, this result for the shadow curve (expressed as χ versus shadow polymer volume fraction ρ_1) is *universal*, i.e. independent of any features of the parent $\rho^{(0)}(L)$ except the presence of a fat tail [83]. The resulting phase coexistence is rather peculiar: at vanishingly small polymer density (and volume fraction), the parent splits off a shadow with a finite polymer volume fraction, and made up of only the very longest chains in the parent. Both phases have vanishingly small pressure; in the shadow, this is achieved by an exact balance between the positive (repulsive) and negative (attractive) contributions to Π.

The reasoning so far gives the onset of phase coexistence which occur as the parent density $\rho_0^{(0)}$ is increased at fixed (sufficiently large) χ. If one wants to find instead the cloud point at fixed non-zero $\rho_0^{(0)}$, caused by an increase in χ, Solc [13, 83] showed that one has to assume that $\lambda \to 0$ as $L_{\max} \to \infty$. This means that the cloud and shadow are 'almost critical': for small chain lengths L (of order the parent average), their density distributions are essentially identical; the shadow only differs from the parent in that it contains a larger fraction of the longest chains ($L \approx L_{\max}$). As a consequence, when represented in a χ versus ρ_1 plot, the cloud and shadow curves actually *coincide* in the limit $L_{\max} \to \infty$; their functional form is again universal and given by $2\chi = 1/(1-\rho_1^{(0)}) = 1/(1-\rho_1)$. However, due to the contribution from the longest chains, all moments $\rho_n = \int \mathrm{d}L\, L^n \rho(L)$ of the shadow with $n > 2$ actually *diverge* with $L_{\max}$; cloud and shadow curves plotted as χ versus ρ_2, for example, would therefore

[1] The strict limit $L_{\max} \to \infty$ is of course unrealizable physically, but useful as a mathematical device for highlighting the effects of large $L_{\max}$.

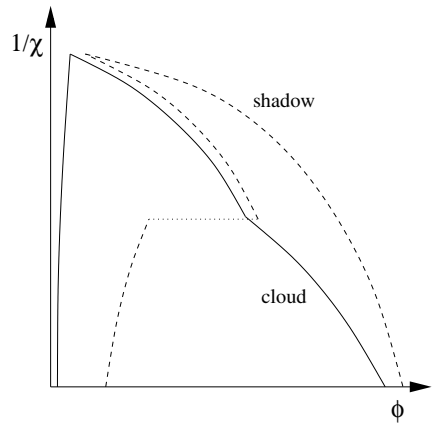

Figure 6. A sketch of cloud and shadow curves for a homopolymer with a fat-tailed length distribution. In the limit where the cut-off $L_{\max}$ on chain lengths becomes very large, the low-density part of the cloud curve becomes vertical, while for polymer volume fractions above zero but below the triple point the cloud and shadow curves approach each other and eventually coincide.

be extremely different (by an infinite amount in the limit). A sketch summarizing the overall shape of the cloud and shadow curves for polymers with fat-tailed length distributions is shown in figure 6.

The above considerations are not as academic as they may seem; log-normal length distributions, for example, have fat tails as defined above and occur frequently in polymer processing. For branched polymers, length distributions with (even fatter) power-law tails arise naturally, and lead to similar phenomena [44].

Flory–Huggins theory is by its nature a mean-field theory; as described above, it is nevertheless rather successful at capturing the effects of length polydispersity on polymer phase behaviour. Close to critical points, deviations will occur; even there, however, polydispersity has been shown to have non-trivial effects. For example, while monodisperse polymers display critical behaviour of the Ising universality class, the critical exponents are modified non-trivially by polydispersity, due to the presence of the large number of conserved densities which act as 'hidden variables' [85].

4.2. Polymers II: Random copolymers

Flory–Huggins theory can also be applied to copolymers, which are made up of random sequences of two types (A and B, say) of monomer. Define σ as the difference between the fractions of A-type and B-type monomer on a chain, such that $\sigma \in [-1, 1]$. One can then have polydispersity in the polymer chain lengths, L, as well as in the chemical chain compositions, σ, and so the system is described by a density distribution $\rho(L, \sigma)$. In the same units as for the homopolymer case, Flory–Huggins theory then gives for the excess free energy

$$\tilde{f} = \frac{1}{L_s}(1-\rho_1)\ln(1-\rho_1) - \chi\rho_1^2 - \chi'\rho_2^2 - \chi''\rho_1\rho_2. \tag{36}$$

Two moment densities enter, defined by the weight functions $w_1(L, \sigma) = L$ and $w_2(L, \sigma) = L\sigma$. I have also included the generalization to a polymeric solvent here, with chain length L_s. As before, χ measures the effective monomer–monomer attraction, but two additional parameters now appear: χ' favours A–B demixing, and χ'' accounts for any asymmetry in the interactions between solvent and monomers A and B, respectively. In the homopolymer

case, where A and B are identical, one has $\chi' = \chi'' = 0$ and then retrieves the expression (29) as expected (up to the term $\chi\rho_1$, which is linear in density and so irrelevant for the phase behaviour).

The case of polydisperse L *and* σ is rather complex, so it is easiest to extract the copolymer-specific effects first by assuming that only the chemical composition σ is polydisperse while the chain length L is monodisperse. One can then make the replacement $\rho(L, \sigma) \to \rho(\sigma)$, and the moment densities ρ_0 and ρ_1 become trivially related according to $\rho_1 = L\rho_0$; similarly, ρ_2 becomes L times the first moment (w.r.t. σ) of $\rho(\sigma)$.

To simplify even further, one can assume that there is no solvent in the system, constraining the polymer volume fraction to $\rho_1 = L\rho_0 = 1$. The normalized σ-distribution is then $n(\sigma) = L\rho(\sigma)$, ρ_2 reduces to the average of σ, and the excess free energy becomes $\tilde{f} = -\chi'\rho_2^2 = -\chi'[\int \mathrm{d}\sigma\, \sigma n(\sigma)]^2$ up to constants and irrelevant linear terms. By adding back some linear terms (and exploiting the fact that $\int \mathrm{d}\sigma\, n(\sigma) = 1$), one can also write this excess free energy as

$$\tilde{f} = \tfrac{1}{2}\chi' \int \mathrm{d}\sigma\, \mathrm{d}\sigma'\, (\sigma - \sigma')^2 n(\sigma) n(\sigma') \tag{37}$$

which shows quite transparently the mechanism of phase separation in this system: phases that contain a spread of different σ can always lower their excess free energy by fractionation; as temperature is lowered, this effect dominates the corresponding loss of entropy of mixing in the ideal part of the free energy, and one expects separation into an ever-increasing number of phases[2]. This remarkable behaviour has indeed been found in numerical calculations [40–42]; an example is shown in figure 7(top). Equally remarkably, one can show that in even such a very simple model system, critical points of arbitrary order can occur (though the required fine-tuning of the parent density distribution would probably make the experimental observation of critical points of higher order than tricritical very difficult) [23].

For the case where solvent is present in the system, but the chain lengths L are still monodisperse, phase coexistences have been calculated in [23]. To simplify matters, the solvent was assumed to be polymeric and to have the same chain length as the copolymer ($L_s = L$). The interaction parameters χ and χ'' were also taken to be zero, with only χ' being non-zero; under these assumptions, the solvent acts exactly like a random copolymer chain with $\sigma = 0$, i.e. composed of equal numbers of A and B monomers. Even for this simple scenario, all symmetric (under $\sigma \to -\sigma$) parent density distributions $\rho^{(0)}(\sigma)$ show a tricritical point at some value of the overall polymer density (see figure 7 (bottom)). This effect generalizes that found in a simpler bidisperse case, where the 'copolymer mixture' only contains the pure A and pure B homopolymers [86, 87]. The fully polydisperse case is nevertheless richer since it also allows critical points of higher order than tricritical.

Finally, the most general case of joint polydispersity in lengths L and chemical compositions σ has been treated by a number of authors (see e.g. [24] for an extensive review). In early work an incorrect form for the excess free energy was used [88, 89]; the correct form is the one given above in equation (36) [42, 90]. While the calculation of phase splits inside the coexistence region remains an open problem, the simpler cloud and shadow curves have been obtained for a number of scenarios. One interesting feature is that even for Schulz distributions of chain lengths, triple points and the associated kinks in the cloud curve are predicted (and observed experimentally [89]). These are clearly due to the chemical polydispersity since homopolymers with Schulz distributions of chain length never exhibit triple points [13, 83].

[2] This phase separation occurs at values of χ' of order $1/L$, rather than of order unity; the reason for this is that the ideal part of the free energy is $\int \mathrm{d}\sigma\, \rho(\sigma)[\ln \rho(\sigma) - 1] = L^{-1} \int \mathrm{d}\sigma\, n(\sigma) \ln n(\sigma)$ (+ linear terms).

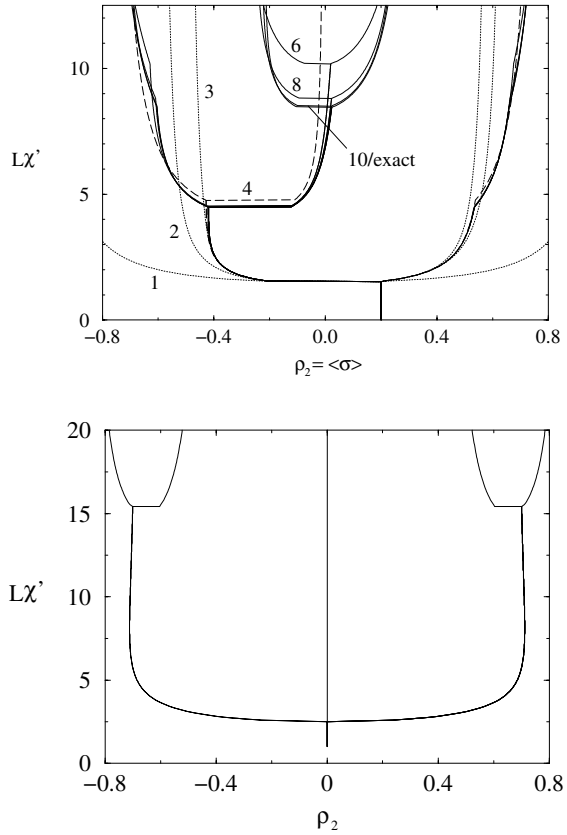

Figure 7. Top: an example of a demixing cascade in a random copolymer blend (i.e. without solvent), as calculated from Flory–Huggins theory [23]. Shown are, for a single parent phase, the values of $\rho_2 = \langle\sigma\rangle$ in the coexisting phases as χ' is increased, corresponding to temperature being decreased. Note how more and more coexisting phases appear, producing new branches of the coexistence curve (connected by horizontal lines to guide the eye). The different curves are calculated using the moment free energy method, and labelled by the number K of moments retained in the description. While the results for the cloud point and shadow are exact even with the smallest K ($K = 1$), the predictions in the coexistence region approach those of an exact calculation as K is increased, and are indistinguishable for $K = 10$. Bottom: with solvent added to the system, parents with appropriately chosen polymer volume fraction exhibit tricritical points, where separation into three infinitesimally different phases occurs [23]. (Only the—essentially exact—results for the largest value of K are shown.)

4.3. Spherical colloids I: Van der Waals theory

Van der Waals theory [17, 63, 91, 92] is the simplest model for the liquid–gas transition, and as such is appropriate for investigating coexistence between gas- and liquid-like phases of colloidal suspensions (in which the structural arrangement of the colloidal particles—for now assumed to be spherical—is analogous to that of the atoms in ordinary gases and liquids). For monodisperse particles, the excess free energy of van der Waals theory is

$$\tilde{f} = -T\rho_0 \ln(1 - b\rho_0) - \tfrac{1}{2}a\rho_0^2.$$

Here the first term represents excluded-volume interactions, i.e. the strong short-range repulsions between colloid particles at and near contact, with the parameter b of the order of the volume of a single particle. The second term, on the other hand, arises from longer-

ranged attractive forces between particles and is of the order of the typical attraction energy times an interaction volume (the latter being again of the order of the particle volume).

In the polydisperse case, $b\rho_0$ is generalized to $\int \mathrm{d}\sigma\, b(\sigma)\rho(\sigma)$ and $a\rho_0^2$ to $\int \mathrm{d}\sigma\, \mathrm{d}\sigma'\, a(\sigma,\sigma')\rho(\sigma)\rho(\sigma')$; the polydisperse attribute σ may represent, for example, the diameter or charge of the colloid particles. The functions $a(\sigma,\sigma')$ and $b(\sigma)$ can be written in a more physically transparent way as

$$a(\sigma,\sigma') = \epsilon(\sigma,\sigma')d^3(\sigma,\sigma') \qquad b(\sigma) = d^3(\sigma,\sigma)$$

where $\epsilon(\sigma,\sigma')$ is the energy scale of attractions between particles with diameter (or charge etc) σ and σ', and $d(\sigma,\sigma')$ is the corresponding interaction length scale. These functions each depend on two arguments, but can be reduced to functions of a single argument if one assumes the so-called mixing rules

$$\epsilon(\sigma,\sigma') = \epsilon^{1/2}(\sigma,\sigma)\epsilon^{1/2}(\sigma',\sigma') \qquad d(\sigma,\sigma') = \tfrac{1}{2}[d(\sigma,\sigma) + d(\sigma',\sigma')]. \tag{38}$$

Abbreviating $\epsilon(\sigma,\sigma)$ to $\epsilon(\sigma)$ and similarly for $d(\sigma,\sigma)$, the excess free energy of polydisperse van der Waals theory is then written as

$$\tilde{f} = -\rho_0 \ln\left(1 - \int \mathrm{d}\sigma\, d^3(\sigma)\rho(\sigma)\right) - \frac{1}{2}\int \mathrm{d}\sigma\, \mathrm{d}\sigma'\, \epsilon^{1/2}(\sigma)\epsilon^{1/2}(\sigma')\left(\frac{d(\sigma)+d(\sigma')}{2}\right)^2 \rho(\sigma)\rho(\sigma') \tag{39}$$

and is seen to have a truncatable structure, depending—for the most general choice of $\epsilon(\sigma)$ and $d(\sigma)$—on six moment densities. These have weight functions 1, $d^3(\sigma)$, and $\epsilon^{1/2}(\sigma)d^n(\sigma)$ $(n = 0, \ldots, 3)$.

Dickinson [17] appears to have been the first to analyse the above model. He used binning into pseudo-components to obtain numerically some results for the ratio of the density distributions in coexisting gas and liquid phases, which indicate the strength of fractionation effects. He also suggested that polydispersity might induce the qualitatively new feature of liquid–liquid demixing, but supposed that deviations from the simple mixing rules (38) are required for this to occur.

Gualtieri *et al* [27] also studied the van der Waals model for simple choices of the σ-dependences, using e.g. a $b(\sigma)$ that was constant or linear in σ, together with $a(\sigma,\sigma')$ = constant or $a(\sigma,\sigma') \propto \sigma\sigma'$. As explained in section 3.3, they used a perturbation theory approach to study the effects of the addition of a small amount of polydisperse material to an otherwise monodisperse system, obtaining the density distributions in coexisting phases and the polydispersity-induced shift in the critical point. For a Schulz parent distribution $(\rho^{(0)}(\sigma) \sim \sigma^\alpha \mathrm{e}^{-\sigma/\sigma_0})$ they also found the full cloud and shadow curves.

Kincaid *et al* [63] also expanded perturbatively, but using the width s of the parent distribution as the small parameter and focusing mainly on the shift in the critical point.

Recently the van der Waals model has been revisited, for parent distributions of Schulz or log-normal form and with various simple choices for the functions $d(\sigma)$ and $\epsilon(\sigma)$ [91]. Cloud and shadow curves were found numerically and showed small but observable changes compared to the monodisperse case for polydispersities s of the order of 10%. For $s \approx 30\%$ and above, new critical points appear, although their thermodynamic stability was not investigated. Further work along these lines [92] also showed that for sufficiently wide (log-normal) parent distributions three-phase coexistence can occur, even for the simple mixing rules (38) above. In fact one can say rather more: if, as in [92], one assumes $d(\sigma)$ = constant—so that the only effect of polydispersity is on the attraction energy parameters $\epsilon(\sigma)$—then in the dense limit the model formally maps to the Flory–Huggins theory of a random copolymer blend [93]

discussed in section 4.2. It can therefore show liquid–liquid demixing into an *arbitrarily large* number of phases as temperature is lowered, and can also exhibit critical points of arbitrarily high order.

4.4. Spherical colloids II: Hard spheres

Van der Waals theory does not address the question of crystallization in colloidal suspensions, where the particles arrange themselves into a lattice structure with long-range translational order. The 'cleanest' system in which to study this transition is one where the colloidal particles act as *hard spheres*, exhibiting no interaction except for an infinite repulsion on overlap. This scenario can indeed be realized experimentally, using for example latex particles that are sterically stabilized by a polymer coating [94]. In a hard-sphere system the only energy scale is set by the temperature; T therefore only appears as a trivial scaling factor in the results and will be set to unity in this section. There is also no gas–liquid transition, so it is common to refer to the non-crystalline phase of hard spheres as a fluid (rather than a gas or a liquid). Monodisperse hard spheres exhibit only a freezing transition, where a fluid with a volume fraction ϕ of spheres of $\phi \approx 50\%$ coexists with a crystalline solid with $\phi \approx 55\%$. Phase separation is observed when the overall volume fraction of the system lies between the values for the coexisting fluid and crystal; for $\phi < 50\%$, on the other hand, one has only the fluid and for $\phi > 55\%$ (and up to the maximum close-packed value of $\phi \approx 74\%$) only the solid.

For colloidal hard spheres, there is inevitably some polydispersity in the diameter σ of the spheres. It was realized early on that such diameter polydispersity might destabilize the colloidal crystal phase, eventually inhibiting freezing above a certain 'terminal' polydispersity. Experimentally, the freezing transition is indeed suppressed in sufficiently polydisperse systems [94, 95]. But the situation is somewhat ambiguous, since the observed terminal polydispersity might also be a non-equilibrium effect due to a kinetic glass transition [96]; the growth kinetics of polydisperse crystals may also cause deviations from equilibrium behaviour [97]. The determination of an accurate *equilibrium* phase diagram for polydisperse hard spheres is nevertheless an important task, if only to allow experimental findings to be properly attributed to equilibrium or non-equilibrium effects. The results could also guide future experiments on colloidal suspensions under microgravity conditions, where—with the glass transition shifted to higher densities or even absent [98]—more of the equilibrium behaviour should be observable. In the remainder of this section, and in keeping with the overall focus of the paper, I will therefore focus on attempts to clarify the *equilibrium* phase behaviour of polydisperse hard spheres.

Much early theoretical work (see [99] for a comprehensive list of references) focused on estimating the terminal value s_t of the polydispersity s. As above, s is defined as the normalized standard deviation of the diameter distribution; see equation (21). Dickinson and Parker [100], for example, extrapolated the decrease of the volume change on melting with polydispersity s to zero, obtaining an estimate of $s_t \approx 30\%$. Pusey [101] used a simple Lindemann-type criterion to estimate that the larger spheres in a polydisperse system would disrupt the crystal structure above $s_t \approx 6 \ldots 12\%$. McRae and Haymet [102] used density functional theory (DFT—see section 5.1) together with the simplifying assumption that there is no fractionation, i.e. that fluid and crystal have the same distribution of diameters, and found that there was no crystallization above $s_t \approx 5\%$. Barrat and Hansen [103] also employed DFT, estimating the free energy difference between fluid and solid; while in the monodisperse case the solid has the lower free energy above volume fraction $\phi = 55\%$, the fluid can become preferred again at large ϕ if the polydispersity s is sufficiently large. This result is compatible with the intuition that polydispersity *reduces* the maximum packing fraction in a crystal (since a range of diameters need to

be accommodated on uniformly spaced lattice sites), while it *increases* the maximum packing fraction in the fluid, where smaller spheres should be able to fill 'holes' between larger particles more easily. A more detailed calculation [99] confirmed this, estimating the terminal polydispersity from the crossing of the maximum packing fractions of liquid and solid as $s_t = 12\%$.

In recent years, computer simulations have also been used to estimate the terminal polydispersity. It is difficult, however, to carry out such simulations for the experimentally most relevant situation of a fixed parental density distribution $\rho^{(0)}(\sigma)$: with a number of particles that can be simulated of the order of hundreds, there will be strong finite-size effects due to the random assignment of diameters to particles; furthermore, with only a few particles in each small range of diameters, it is almost impossible to ensure that the size distributions in coexisting phases are properly equilibrated. Instead, a semi-grandcanonical approach has been used, which prescribes the differences in chemical potential $\mu(\sigma)$ between different σ; effectively, one then simulates a system with variable polydispersity. Bolhuis and Kofke, for example, imposed a parabolic shape for the chemical potential differences, giving a Gaussian distribution of diameters at low density [104]. Using thermodynamic integration they then followed the pressure at which fluid–solid coexistence occurs as a function of the width of this Gaussian distribution. They found that this coexistence line terminates, at a point where the densest packings for fluid and solid were reached; the diameter distributions there were significantly different, with the fluid having a polydispersity of $s \approx 12\%$ and the solid $s \approx 6\%$. However, this terminal point is of limited relevance, since it only exists *for the given chemical potential differences*. One can in fact go beyond it by considering more general functional forms for the chemical potential differences [105]; nevertheless, Kofke and Bolhuis observed that the coexisting solid always seemed to have a polydispersity below $s \approx 6\%$, while for the fluid much larger values of s could be reached. (An unpublished preprint by Almarza and Enciso [106] comes to similar conclusions.) Based on this observation, it was suggested [105] that a polydisperse hard-sphere fluid may freeze by splitting off a series of solids each comprising a narrow range of (large) sphere diameters[3].

While the simulation results described above are suggestive, they are still obtained for variable polydispersity, i.e. by fixing chemical potential differences. In contrast to the experimental situation, the overall particle size distribution can thus change (sometimes dramatically) across the phase diagram, limiting the applicability of the results[4]. A number of researchers have therefore tried to investigate the phase behaviour of polydisperse hard spheres theoretically, using approximate expressions for the (excess) free energy. For the fluid phase, the most accurate such approximation available is currently believed to be the generalization by Salacuse and Stell [20] of the BMCSL equation of state [109, 110]; for the monodisperse case this reproduces the well-known Carnahan–Starling equation of state. Assuming that sphere diameters are measured in units of some reference value σ_0, and that all densities are made non-dimensional by multiplying by the volume $\pi\sigma_0^3/6$ of a reference sphere, the BMCSL expression for the excess free energy is

$$\tilde{f} = \left(\frac{\rho_2^3}{\rho_3^2} - \rho_0\right)\ln(1-\rho_3) + \frac{3\rho_1\rho_2}{1-\rho_3} + \frac{\rho_2^3}{\rho_3(1-\rho_3)^2}. \tag{40}$$

This has again a truncatable form, involving only the (ordinary) moments $\rho_i = \int \mathrm{d}\sigma\, \sigma^i \rho(\sigma)$ ($i = 0, \ldots, 3$) of the density distribution; with our choice of units, $\rho_3 \equiv \phi$ is the volume fraction of spheres. Bartlett [111] provided an elegant argument for why—at least within a

[3] In a more extreme scenario, where the diameter distribution has a fat (slower than exponential) tail extending to very large values, Sear [107] argued that such a fractionated solid would in fact occur already at vanishingly small densities.

[4] A simulation technique for addressing this problem is currently being developed [108].

virial expansion—such a moment structure of the excess free energy for the hard-sphere fluid should in fact be exact[5].

For phase coexistence calculations it is desirable also to have a compact expression for the excess free energy of the polydisperse hard-sphere *crystal*. This is not at all a trivial question, in particular since the structure of such a crystal could be rather complex, with different sites inside the crystalline unit cell occupied preferentially by particles with different ranges of diameters. Most theoretical work therefore assumes that one instead has a substitutional solid, where crystal sites are occupied equally likely by particles of any diameter. A simple-minded but popular approach to estimating the free energy is then cell theory, where particles are treated as independent but confined in an effective cell formed by their neighbours (see e.g. [116]). A more quantitative, 'geometric' approach has recently been proposed by Bartlett [111, 117]: he assumed that the excess free energy of the solid depends on the same moment densities ρ_0, $\ldots$, ρ_3 as that of the fluid, and then fitted the functional form of this dependence by comparing with simulation data on bidisperse hard-sphere systems.

By applying the moment free energy method to the BMCSL free energy for the fluid and Bartlett's 'geometric' free energy for the solid, Bartlett and Warren [118] recently investigated the freezing behaviour of polydisperse hard spheres. They found that the range of volume fractions where fluid–solid coexistence is observed narrows as the polydispersity s is increased and eventually shrinks to zero at a terminal polydispersity $s_t \approx 8\%$. (At this point, the density distributions in the fluid and solid were calculated to be equal, but as the symmetries of the two phases are different this is not a critical point but rather a 'point of equal concentration' [118].) At values of s just below s_t, they also found a transition to a re-entrant fluid at large volume fractions (see figure 8 (left)). Such a re-entrance is in fact to be expected from the earlier work on the terminal polydispersity described above: for sufficiently polydisperse systems, the fluid should at large volume fractions be thermodynamically preferred over the solid because it packs the spheres more efficiently. When interpreting the results of [118], however, it needs to be borne in mind that the approximations made in effect constrained the polydispersity (normalized standard deviation) s to be equal in the coexisting fluids and solids, allowing only the mean sizes to be different. The possibility of a very polydisperse fluid splitting off a solid containing a narrow range of diameters is thus disallowed. Work is in progress to remove these simplifications [93], and one may speculate that the point of equal concentration would disappear in a more accurate treatment (see figure 8(right)).

The analysis of the freezing behaviour of strongly polydisperse hard spheres is complicated by the fact that, instead of a single solid phase, a number of coexisting solids with strong diameter fractionation between them may appear. Bartlett [119] and Sear [116] both investigated this possibility, using different approximations for the free energy for the solid, and found that an increasing number of fractionated solids should appear as the system is made more polydisperse. Both calculations only compared the free energies of the liquid and the fractionated solids, however, rather than solving the full phase equilibrium conditions. They also used the drastic assumption that the different solids would split the range of diameters evenly between themselves, so that spheres of any given diameter would occur in only a single phase; in reality, one would expect a rather more gradual fractionation of the phases.

One final complication in the phase behaviour of strongly polydisperse hard-sphere fluids is the possibility of fluid–fluid demixing. While for *bidisperse* hard spheres such a demixing transition is believed to be absent (or at least always metastable compared to the freezing transition), Warren [38] found, using the BMCSL free energy, that for a bimodal diameter

[5] Within the so-called 'mean-spherical approximation', truncatable free energies have recently also been found for adhesive or 'sticky' hard spheres [112–115]; these are models of spherical colloids which, in addition to a hard repulsion on contact, interact via strong short-range attractive forces.

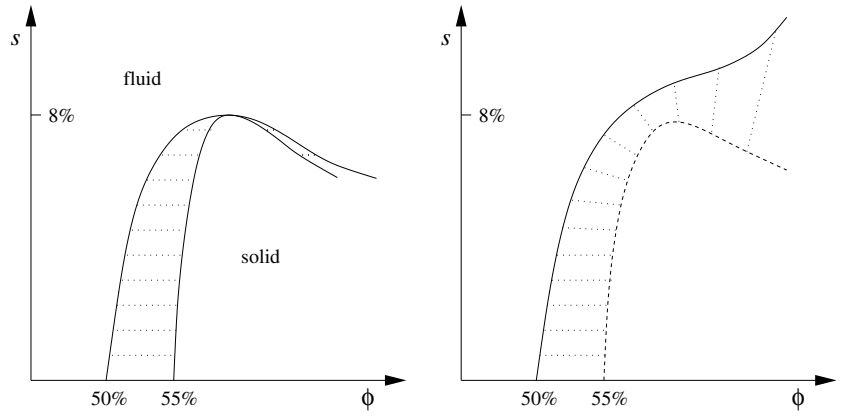

Figure 8. Left: a sketch of Bartlett and Warren's phase diagram for polydisperse hard spheres [118]. Shown is the result of their simplest approximation, in which fractionation is not allowed; cloud and shadow curves then effectively reduce to the conventional coexistence curves for monodisperse systems, and coexisting phases (connected by dotted lines) share the same value of the polydispersity s. (A better approximation used in [118] allowed fractionation but still effectively constrained s to be equal in coexisting phases.) Note the re-entrant transition to a fluid at large colloid volume fraction ϕ, for polydispersities s just below the terminal value $s_t \approx 8\%$. At s_t, the phase boundaries meet in a 'point of equal concentration'. Right: the possible shape of the 'true' phase diagram that would result from a calculation which allows for different polydispersities of fluid and solid. Shown are a cloud curve from the fluid side, and the corresponding curve of solid shadow phases; coexisting phases are again connected by dotted lines. There is now no reason that cloud and shadow curves should meet, so a point of equal concentration seems unlikely. There may also not be a terminal value of the polydispersity on the fluid cloud curve, since even a very polydisperse fluid may always be able to split off a solid with a narrow distribution of particle diameters. At large values of s, fluid–fluid demixing (not shown) might pre-empt the fluid–solid transition.

distribution a demixing instability could occur at reasonable volume fractions. Warren noticed that significant polydispersity ($s \geqslant 50\%$) in the larger spheres was necessary to produce this effect. He conjectured that the demixing occurred because the smaller spheres cause an effective attraction (depletion interaction; see section 4.5 below) between the larger spheres; polydispersity then facilitates the demixing by making a dense phase of larger spheres more favourable (due to the increased maximal packing fraction). Cuesta [29] studied log-normal diameter distributions; even though these only have a single maximum, and thus no separation into small and large spheres akin to the bimodal case, he still predicted fluid–fluid demixing for large polydispersities ($s \geqslant 160\%$).

The theoretical studies reviewed above still leave open a substantial number of questions. For fluid–fluid demixing, for example, only the spinodal instability was analysed [29,38]. The actual demixing transition will occur at a lower density yet to be determined; and no predictions exist for the freezing behaviour of such demixed fluids at higher densities. The drastic—and differing—approximations for size fractionation that were used in the studies of re-entrant melting and solid–solid coexistence [116,118,119] also leave the relative importance of these two phenomena unclear. Work is now under way to address these questions and produce a coherent picture of the equilibrium phase behaviour of polydisperse hard spheres [93].

4.5. Colloid–polymer mixtures

Moving beyond suspensions of (hard-) spherical colloids alone, colloid–polymer mixtures have in recent years attracted considerable interest, mainly because the polymer induces an easily tunable 'depletion interaction' between the colloids. This interaction arises as follows. When colloidal particles approach each other to within twice the radius of gyration (i.e. the

effective diameter) of the polymer chains, they form a 'depletion zone' between them which the polymer chains cannot enter. The result is an imbalance in the polymer osmotic pressure which pushes the colloidal particles together, causing an effective colloid–colloid attraction. This attraction can lead to the appearance of a (colloidal) gas–liquid coexistence region in the phase diagram [120]; its range and strength are tunable via the size of the polymer chains and the polymer concentration, respectively. This feature makes colloid–polymer mixtures interesting model systems with which to study the conditions required for the appearance of liquid phases; theory, simulation, and experiment all reveal, for example, that the interaction range needs to exceed a certain fraction of the particle size (of order 30%) in order for gas–liquid coexistence to be stable rather than metastable [120–122].

To model the simplest case of colloids with hard interactions and ideal polymers (in a so-called θ-solvent), the Asakura–Oosawa model [123] has been widely used. It treats the polymer coils as spherical particles that can interpenetrate freely with each other, but experience a hard-sphere repulsion when they come into contact with the colloids. Formally integrating out the polymer degrees of freedom then results in the expected attractive colloid–colloid interaction. However, this interaction generally contains many-body terms (arising from the overlap of the depletion zones of more than two colloids) [122] and so its effect is difficult to take into account exactly. But progress can be made using a van der Waals (mean-field) type of approach which replaces the effective colloid–colloid interaction by its average over the pure (hard-sphere) colloid system [121]. In the case of monodisperse colloid, the resulting phase behaviour is well understood, with the main feature being the appearance of gas–liquid phase separation; non-ideality of the polymer chains can also be included in the model but only introduces a weak temperature dependence into the phase behaviour [124]. Polydispersity in polymer chain lengths has been studied [125, 126], but only for variable polydispersity where the chemical potential differences between chains of different length are imposed. Warren [127] considered instead the experimentally more relevant situation where the overall polymer density distribution is imposed, in the simpler case where the polymer consists of a binary mixture of chains of two different lengths. He made the intriguing observation that polydispersity has almost no effect on the phase behaviour as long as the polymer concentration is expressed in terms of an effective volume fraction (which allocates to each polymer chain a volume proportional to the cube of its radius of gyration). The generalization to a fully polydisperse polymer with imposed density distribution is challenging, but work in this direction is in progress [93].

The results reviewed above all concern the case of colloidal particles of identical size. For the more complicated case of polydisperse colloids, only rough qualitative estimates of the effects on phase behaviour [128] and limited perturbative results for narrow size distributions [67] exist. Recent experimental results [128] do, however, suggest that for fully polydisperse colloids intricate—and largely unexplored—phase diagram topologies may occur, due to the combination of gas–liquid coexistence on the one hand and re-entrant melting in the absence of polymer on the other. The theoretical analysis of these effects remains an open problem, but should be helped by the fact that, even for the most general case of polydisperse colloid diameters *and* polydisperse polymer chain lengths, the van der Waals treatment of [121] leads to a truncatable structure for the free energy [93].

4.6. Colloidal liquid crystals I: Maier–Saupe theory for thermotropics

So far I have only discussed spherical colloids. Non-spherical particles, shaped e.g. like rods or plates, can form liquid crystalline phases; these are the subject of the following sections. One of the simplest liquid crystal structures is the nematic. Like a liquid, it has no long-range translational order, but the rods are *orientationally* ordered, pointing preferentially along a

fixed direction called the nematic axis. The density distribution required to describe a nematic phase of length-polydisperse rod-like particles thus depends on two variables, the rod length and the rod orientation. Since the orientation of a rod can and will change over time, one has a mixture of conserved and non-conserved degrees of freedom, and this makes the problem rather challenging.

Liquid crystals in which phase transitions are driven primarily by changes in temperature (rather than density) are called *thermotropic*. The standard model for analysing their phase behaviour is Maier–Saupe theory [129], which captures the orientation-dependent attractions between particles. It was originally derived on the basis of an approximate treatment of the van der Waals attraction between large molecules, caused by fluctuating charge densities in their electron clouds, but is actually much more widely applicable as a phenomenological theory of orientation-dependent interparticle attractions.

Consistent with the physical intuition that in thermotropics phase transitions are driven by temperature variations rather than changes in density, Maier–Saupe theory effectively neglects changes in the overall particle density, so that different phases only differ in their normalized distributions $n(L, \Omega)$ over rod lengths L and orientations Ω. With the density having been fixed, it is sensible to switch from the free energy density $f = F/V$ to the free energy per particle F/N as the basic quantity from which to analyse phase behaviour; the non-ideal part of this is, for Maier–Saupe theory

$$\frac{\tilde{F}}{N} = -\frac{1}{2}\int \mathrm{d}L\,\mathrm{d}L'\,\mathrm{d}\Omega\,\mathrm{d}\Omega'\,n(L,\Omega)n(L',\Omega)u(L,L')P_2(\cos\theta)P_2(\cos\theta'). \tag{41}$$

The main ingredient of this expression is the angular dependence through the second-order Legendre polynomials $P_2(\cos\theta) = (3\cos^2\theta - 1)/2$; here θ is the angle of a rod with the nematic axis. The excess free energy (41) favours nematic ordering, as it would be minimal if all rods pointed along the nematic axis ($\theta = 0$). The ideal part $T\int \mathrm{d}L\,\mathrm{d}\Omega\,n(L,\Omega)[\ln n(L,\Omega) - 1]$ of the free energy per particle instead prefers an isotropic phase (which, due to its random rod orientations, has the largest orientational entropy).

In the monodisperse case, where there is only a single rod length L, Maier–Saupe theory leads to a transition from an isotropic to a nematic phase as the temperature is lowered. This is consistent with the intuition explained above; the scale for the transition temperature is set by the energy scale for the attractive interaction, $u(L, L)$. Note that there is no coexistence gap here, i.e. no temperature region where isotropic–nematic (I–N) phase coexistence is observed. This is because the only conserved density is the total particle density, which is assumed equal in all phases.

In the polydisperse case, the (essentially phenomenological) function $u(L, L')$ determines how the strength of the attraction varies with the rod lengths. Now there are non-trivial conserved densities: the length distribution $n^{(0)}(L)$ of the parent phase has to be maintained, and the system may be able to lower its free energy by separating into two phases with different length distributions. Accordingly, Sluckin [130] found in a perturbative calculation for narrow polydispersity that a coexistence gap develops in the polydisperse system; the temperature range over which I–N coexistence is observed is proportional to the variance s^2 of the parent length distribution. Since the function $u(L, L')$ is of a phenomenological nature, the same conclusion also applies if the polydisperse attribute is different, e.g. rod diameter or charge instead of length.

The effects of stronger polydispersity (which cannot be treated perturbatively) in the Maier–Saupe model remains unexplored; one interesting question that could be asked [131] is whether coexistence between several nematic phases would eventually develop, as it does in the Onsager model discussed next.

4.7. Colloidal liquid crystals II: isotropic–nematic transition in hard rods

In *lyotropic* liquid crystals, the important control parameter causing phase transitions is density, rather than temperature as in thermotropics. The paradigmatic model for lyotropic colloidal liquid crystals is that of Onsager [132], which neglects any long-range attractions between particles and only retains the short-range repulsions; the latter are taken to be hard (infinite repulsion on contact). Rod-like colloidal particles approximating closely such 'hard rods' can be realized experimentally (see e.g. [133]). Because of the hard interactions in the Onsager model, the temperature can be trivially scaled out of all results and will be set to unity below.

Onsager's treatment of the hard-rod model is based on a virial expansion in the overall particle density. Crucially, it turns out that for long thin rods, and in the region of densities where the I–N phase transition occurs, this virial expansion can be *exactly* truncated after the first non-trivial (second virial) contribution. The intuitive reason for this is as follows. Assume the rods have cylindrical shape, with length L and diameter D. Any given rod excludes another, randomly oriented rod from a volume of $\mathcal{O}(L^2D)$. The I–N transition occurs at densities ρ_0 where the number of rods in this excluded volume becomes of order one, giving $\rho_0 \sim L^{-2}D^{-1}$. Multiplying by the rod volume ($\sim LD^2$) gives the rod volume fraction $\phi \sim D/L$ at the transition. For long thin rods this becomes vanishingly small, making it plausible that higher-order terms in the virial expansion can be neglected.

To state the free energy of a system of long thin rods with polydisperse lengths L and diameters D, let us choose a reference length L_0 and reference diameter D_0, and define normalized lengths $\tilde{L} = L/L_0$ and diameters $\tilde{D} = D/D_0$. It is conventional to choose $(\pi/4)L_0^2D_0$ as the unit volume to make densities non-dimensional; this is the average excluded volume of two randomly oriented reference rods. In the Onsager limit $D_0/L_0 \to 0$ (at fixed distribution of $\tilde{L}$ and $\tilde{D}$), the excess free energy of this hard-rod system then becomes [134]

$$\tilde{f} = \frac{4}{\pi}\int \mathrm{d}\tilde{L}\,\mathrm{d}\tilde{L}'\,\mathrm{d}\tilde{D}\,\mathrm{d}\tilde{D}'\,\mathrm{d}\Omega\,\mathrm{d}\Omega'\,\rho(\tilde{L},\tilde{D},\Omega)\rho(\tilde{L}',\tilde{D}',\Omega')\tilde{L}\tilde{L}'\frac{\tilde{D}+\tilde{D}'}{2}|\sin\gamma(\Omega,\Omega')|. \quad (42)$$

The non-trivial factors in this expression arise from the fact that the excluded volume of two rods making an angle γ with each other is $LL'(D+D')|\sin\gamma|$, or $(4/\pi)\tilde{L}\tilde{L}'(\tilde{D}+\tilde{D}')|\sin\gamma|$ in our volume units. The excess free energy is a functional of the density distribution $\rho(\tilde{L},\tilde{D},\Omega)$, which is defined such that $\rho(\tilde{L},\tilde{D},\Omega)\,\mathrm{d}\tilde{L}\,\mathrm{d}\tilde{D}\,\mathrm{d}\Omega$ is the density of rods with lengths in an interval $\mathrm{d}\tilde{L}$ around $\tilde{L}$, diameters in an interval $\mathrm{d}\tilde{D}$ around $\tilde{D}$, and orientations in a solid angle $\mathrm{d}\Omega$ around Ω.

If the orientation Ω is parametrized in terms of the rod angle θ with the nematic axis, and the azimuthal angle φ, then the density distributions are independent of φ and the integrations over φ and φ' in (42) can be carried out, defining a function

$$K(\theta,\theta') = \frac{4}{\pi}\int \mathrm{d}\varphi\,\mathrm{d}\varphi'\,|\sin\gamma(\Omega,\Omega')| \quad (43)$$

which encodes the angular dependence of the excluded-volume interaction.

For the case of monodisperse rods (see [134] for a comprehensive review), one sets $\tilde{D} = \tilde{D}' = 1$ and $\tilde{L} = \tilde{L}' = 1$ everywhere in (42); the density distribution then becomes a function $\rho(\theta)$ of only the rod angle θ with the nematic axis. One can separate this into its conserved and non-conserved parts by writing $\rho(\theta) = \rho_0 n(\theta)$; the normalized orientation distribution function $n(\theta)$ is found for any given ρ_0 by minimizing the free energy. This gives, at least conceptually, the free energy as a function of ρ_0; a double-tangent construction then shows a coexistence gap, across which an isotropic phase of density $\rho_0 \approx 3.29$ coexists with a nematic phase with $\rho_0 \approx 4.19$.

Consider now the case of length polydispersity (with the diameters still monodisperse). Previous work in this area has focused on the simplified case of bi- and tridisperse mixtures

(rods with two or three different lengths) and has uncovered—for sufficiently disparate lengths—a number of features not observed in the monodisperse case. These include the possibility of coexistence of several nematic phases (N–N), possibly also together with an isotropic phase (I–N–N) [135–139]; such an I–N–N coexistence has indeed been observed experimentally [133]. In the tridisperse case [140], up to four phases (I–N–N–N) can coexist. For bidisperse systems with length ratios above ≈ 5, re-entrant phase coexistence sequences such as I $\rightarrow$ I–N $\rightarrow$ N $\rightarrow$ I–N $\rightarrow$ N are also found [135]. At rod volume fractions far above the onset of I–N coexistence (but, due to the Onsager limit $D_0/L_0 \rightarrow 0$, still negligible compared to unity), the phase diagram is predicted to be density independent, with the result that N–N coexistences persist rather than being terminated by a critical point at high density [137, 138, 140]. For bidisperse *diameters* and monodisperse lengths, I–I demixing [141, 142] and I–I–N coexistence can occur as additional features; a nice discussion on why multiple isotropic phases require diameter polydispersity can be found in [142].

The studies described above show that a wealth of new phase behaviour can result even for bidisperse hard-rod systems. For the potentially even richer case of true polydispersity, however, results to date are very limited. The only studies of the full Onsager model are perturbative calculations, which show a widening of the coexistence gap at the I–N transition [130, 143] with increasing length polydispersity[6]. For the simpler Zwanzig model of rods oriented along one of three perpendicular axes, a full treatment of the length polydisperse case [70] has recently confirmed this trend. However, no evidence of N–N coexistence was found, even for significant polydispersities; an earlier calculation for the bidisperse case gave similar results [144]. This contrast to the predictions of the full Onsager model can be explained intuitively as follows: when a polydisperse nematic phase splits into two nematics containing predominantly short and long rods, respectively, it gives up entropy of mixing but gains orientational entropy. In the Onsager model, where the rod angles are continuous variables, the gain in orientational entropy can be arbitrarily large, thus favouring such a phase split. (The orientational entropy tends to $-\infty$ as the orientational distribution function tends to a delta function.) In the Zwanzig case, on the other hand, the maximum gain in orientational entropy is $k_B \ln 3$ (this being the difference between the entropies of an isotropic and a fully ordered nematic phase), so nematic–nematic coexistence is disfavoured.

It is clear, then, that a number of open questions remain regarding the effects of polydispersity in the Onsager model of hard rods. In particular, one would like to know under which conditions on the width and/or shape of the length and diameter distributions, N–N, I–N–N, and I–I phase coexistences are possible. The answers cannot be inferred from the results for the bi- or tridisperse cases; otherwise one would incorrectly predict, for example, that any polydisperse system should show N–N coexistence since it contains *some* rods of very different lengths. Equally, it remains unclear how many nematic phases can coexist far above the I–N transition, where the phase diagram becomes density independent. Genuine polydispersity could also cause entirely new effects, e.g. demixing into more than two isotropic phases for sufficiently wide diameter distributions.

Tackling the polydisperse Onsager model head on is difficult, since the excess free energy (42) does not have a truncatable structure. However, one can exploit the known

[6] Chen's analysis [143] provides an instructive example of the importance of taking fractionation into account when studying polydisperse phase behaviour. The coexistence region for a parent phase with a given length distribution is bounded by the isotropic cloud point—where the nematic phase first appears—at the lower end, and the nematic cloud point—where the fractional volume occupied by the isotropic phase goes to zero—at the upper end. Chen instead found the densities of the isotropic cloud phase and its coexisting shadow. The gap between these two densities *decreases* as polydispersity increases, while the width of the coexistence region *increases*.

expansion of the angular part $K(\theta, \theta')$ of the excluded-volume interaction (see (43)) in terms of Legendre polynomials. This takes the form [145]

$$K(\theta, \theta') = c_0 - \sum_{n=1}^{\infty} c_n P_{2n}(\cos\theta) P_{2n}(\cos\theta') \tag{44}$$

with positive constants c_n. Truncating this series at successively higher order, one recovers truncatable systems which approach the full Onsager model in the limit; the moment densities that occur are defined by the weight functions $w_n(\tilde{L}, \tilde{D}, \theta) = \tilde{L} P_{2n}(\cos\theta)$ (as well as $\tilde{L}\tilde{D} P_{2n}(\cos\theta)$ if diameter polydispersity is present). Judging from existing work on the monodisperse case [135], even the lowest non-trivial order of truncation—which, for length polydispersity, gives one conserved and one non-conserved moment density—should already give qualitatively correct results [131].

4.8. Colloidal liquid crystals III: Hard rods at higher densities

Rod-like colloidal particles should, at sufficiently high densities, form crystalline solids; a smectic phase (where the particles are arranged into layers that are perpendicular to their preferred orientation, but lack translational order within the layers) may also intervene between the nematic and the crystal phase. Neither smectic nor crystal phases are accessible within the Onsager theory of long thin rods as outlined above, however: they occur at rod volume fractions of order unity, and hence densities $\rho_0 \sim L^{-1}D^{-2}$; the densities $\rho_0 \sim L^{-2}D^{-1}$ at the isotropic–nematic transition are much smaller (in fact infinitely so, in the Onsager limit $D/L \to 0$).

Studying the effects of polydispersity in this high-density regime is an enormous challenge, in part because there is still significant controversy over the most appropriate free energy functionals in this region of the phase diagram [146–148]. Some qualitative features are known, however. Significant length polydispersity, for example, should make smectic (and possibly also crystalline) phases less favourable, since a broad range of rod lengths will be difficult to accommodate within these structures. Instead, one expects to see columnar phases, where the rods are arranged into columns which are themselves packed into a two-dimensional hexagonal lattice; since the rods can slide freely within each column, such columnar phases can easily tolerate a spread of rod lengths. Sluckin [130] indeed found, within a perturbative treatment, that the onset of smectic order should be delayed (i.e. shifted to higher densities) by polydispersity in rod lengths, and that eventually the smectic phase should disappear in favour of a columnar phase. Bates and Frenkel [146] arrived at similar conclusions from their semi-grandcanonical (variable polydispersity) simulations: when the polydispersity increased beyond a terminal value of $s \approx 18\%$, the smectic phase was no longer stable. They also argued that length polydispersity should destabilize the crystal in favour of the columnar phase, though disagreeing on the density dependence of the relative stability of the two phases with an earlier density functional treatment [147].

One final new effect of length polydispersity on hard-rod phases at high densities is the possibility that, on increasing the density, nematic–nematic demixing might occur before the transition to a smectic or columnar phase [149]. This seems entirely plausible, given that the Onsager treatment described above predicts N–N demixing (in sufficiently bidisperse systems) at densities arbitrarily far above the I–N transition. The behaviour of such demixed nematics at higher densities is an entirely open question; they might, for example, form two demixed (fractionated) smectics rather than a single columnar phase. Another area that remains unexplored is the effect of *diameter* polydispersity on the high-density behaviour: this would be expected, for example, to disadvantage columnar phases against smectics, thus producing

an effect opposite to that of length polydispersity.

4.9. Colloidal liquid crystals IV: Plates and rod–plate mixtures

Liquid crystalline phases can also occur in suspensions of *plate-like* (rather than rod-like) particles. If the particles have hard interactions and are monodisperse, then one expects the sequence isotropic (I) → nematic (N) → columnar → crystalline as the particle density is increased. As for rod-like particles, the I–N transition (observed experimentally in [150]) can be analysed using Onsager's second virial theory, although due to the different scaling of the higher-order virial coefficients the results do not become exact even in the limit of very thin plates.

The effect of polydispersity on the phase behaviour of plate-like colloids is only just beginning to be understood. Computer simulations of thin hard plates with polydisperse diameters have shown, for example, that the isotropic–nematic coexistence gap widens with polydispersity [151]. (Though the usual caveat applies regarding the results of semi-grandcanonical simulations, which address the case of variable rather than fixed polydispersity.) The fractionation of plate *diameters* between I and N phases was observed to be rather weak. Plates with polydisperse *thicknesses*, on the other hand, displayed strong fractionation in experiments on the I–N transition [152].

At higher densities, experiments have shown the columnar phase to be remarkably robust against polydispersity in plate diameters [153], tolerating polydispersities up to $s \approx 25\%$. On further increasing the density, a crossover to smectic ordering was observed; this seems plausible, since a spread in particle diameters should prevent an efficient packing of the columns of particles at high densities, favouring instead the layered structure of a smectic.

The addition of non-adsorbing polymer produces further interesting features in the phase behaviour of polydisperse platelets. Experimentally, a strong widening of the isotropic–nematic coexistence gap was observed [152], along with the occurrence of two separate isotropic phases. The latter effect seems to be similar to the 'splitting' of the hard-sphere fluid into a gas and a liquid by the addition of polymer.

Even more complex phase behaviour, finally, can occur in mixtures of rod- and plate-like colloidal particles. Recent experiments [154, 155] show dramatic polydispersity effects: up to five coexisting phases are found, rather than the maximum of three expected for monodisperse hard rods and plates.

Most of the above results for systems involving plate-like colloids remain poorly understood theoretically; open questions include, for example, the contrasting effects of diameter and thickness polydispersity at the I–N transition (especially as regards fractionation), and the precise topologies of the phase diagrams for plate–polymer and plate–rod mixtures. At least for the phenomena involving isotropic and nematic phases, progress should be possible using second virial theories of the Onsager type; if the angular dependences are truncated as described after equation (44), free energy expressions with a truncatable structure will result and can be studied using for example the moment free energy method.

5. Outlook

Throughout this review, I have focused entirely on equilibrium bulk phase behaviour. Beyond this, there are significant open challenges in understanding the effects of polydispersity on inhomogeneous phases and on phase transition kinetics.

5.1. Inhomogeneities

Inhomogeneities come to the fore when one is interested in, for example, the behaviour of a polydisperse material near an interface or a wall; one might want to calculate e.g. the effect of polydispersity on interfacial tensions or other interfacial thermodynamic properties. The description of an inhomogeneous system requires a particle density distribution $\rho(\boldsymbol{r}, \sigma)$ which depends not only on the polydisperse attribute σ but also on the spatial location $\boldsymbol{r}$; the density distribution $\rho(\sigma)$ used above to describe the state of bulk materials is found from this by integration over the sample volume, $\rho(\sigma) = \int \mathrm{d}\boldsymbol{r}\, \rho(\boldsymbol{r}, \sigma)$. In dependence on $\rho(\boldsymbol{r}, \sigma)$ one can again define a free energy $f([\rho(\boldsymbol{r}, \sigma)])$—conventionally referred to as a 'density functional'—that assumes its minimal value at the equilibrium density distribution $\rho(\boldsymbol{r}, \sigma)$ (see e.g. [156, 157] for reviews of density functional theory).

In principle this approach can also be used to obtain from first principles the free energy of bulk phases with spatial ordering, such as hard-sphere crystals: to get the free energy $f([\rho(\sigma)])$ that I have used throughout this paper, one would have to minimize $f([\rho(\boldsymbol{r}, \sigma)])$ over all $\rho(\boldsymbol{r}, \sigma)$ with the given $\rho(\sigma) = \int \mathrm{d}\boldsymbol{r}\, \rho(\boldsymbol{r}, \sigma)$. With orientational degrees of freedom included appropriately, the same method would also apply e.g. to the smectic, columnar and crystalline phases of rod- and plate-like colloids. In practice, this programme can of course only be implemented very approximately: to start with, the full free energy functional $f[\rho(\boldsymbol{r}, \sigma)]$ is not known exactly; and the minimization over the spatial density distribution can normally only be carried out over a small number of assumed candidate structures, parametrized by appropriate variational parameters.

What, then, are the specific challenges in the treatment of inhomogeneities that arise from the presence of polydispersity? Firstly, there is the problem of how to incorporate polydispersity into the construction of approximate density functionals. For polydisperse hard spheres, some significant progress in this direction has been made recently by Pagonabarraga *et al* [158], exploiting again a moment structure for the excess part of the free energy: the moments ρ_i then generalize to spatially varying densities $\rho_i(\boldsymbol{r})$, defined as local averages of the full density distribution $\rho(\boldsymbol{r}, \sigma)$. For spatially extended objects such as polymers, the most appropriate way of carrying out the local averaging is by no means obvious [159]; a recent proposal models the polymers as interpenetrable particles with a fixed monomer density profile about their centre, chosen to reproduce the correct structure factor for ideal polymer chains [160].

The second challenge is to use density functionals for polydisperse systems in practical calculations of interfacial properties, etc. When the excess free energy has a dependence only on certain spatially varying moment densities $\rho_i(\boldsymbol{r})$, this can be done relatively efficiently: the problem then effectively reduces to that of a conventional density functional theory for a discrete mixture of quasi-species [158, 160].

5.2. Phase separation kinetics

The kinetics of phase separation in polydisperse systems is a very challenging and to a large extent unsolved problem. Above, we have seen that the description of equilibrium phase behaviour can be substantially simplified through the use of moment densities; a natural question to ask is then whether moment densities remain useful in understanding the kinetics of phase separation. Warren [159] has in fact argued that in many systems the zeroth moment (total particle density) ρ_0 should relax much more rapidly—by collective diffusion—than can the higher moments, whose equilibration requires interdiffusion of different particle species. This leads to the hypothesis that phase separation could proceed in two stages: in the first

stage, only the densities of coexisting phases would equilibrate, while their compositions would remain equal ('quenched') to that of the parent phase; the kinetics in the second stage would be much slower and bring the compositions of the phases to equilibrium by fractionation. Of course, the onset of phase coexistence with all compositions quenched will generally occur at a different point in the phase diagram compared to the case where full fractionation is allowed. Experimentally observed cloud and shadow curves, for example, could therefore be quite strongly dependent on the timescale of a phase separation experiment, probing behaviour ranging from the quenched to the fully fractionated phase diagram.

In principle, it is of course possible to treat the phase separation kinetics in polydisperse systems by binning the range of the polydisperse attribute σ, reducing the problem to the dynamics of a finite mixture of discrete species. In general one expects this approach to be infeasible numerically; Clarke [161] has recently shown, however, that it can be efficiently implemented to study the early stages of phase separation of polydisperse polymers which are suddenly cooled into a two-phase region of their phase diagram.

Finally, there is the intriguing possibility that the kinetics of phase separation (and, in particular, fractionation) in polydisperse systems could be so slow as to make the equilibrium phase behaviour unobservable in practice. Evans and Holmes [97] have recently argued that this is the case for polydisperse hard-sphere crystals: once particles are incorporated into a crystal nucleus growing from the hard-sphere fluid, they essentially no longer diffuse on experimental timescales. The size distribution of particles in the crystal will thus be 'frozen in', and determined by the mechanism of crystal growth rather than the conditions of thermodynamic equilibrium. A full understanding of such non-equilibrium effects on the experimentally observed phase behaviour of colloidal systems remains a significant challenge for future work.

6. Conclusions

In this review, I have attempted to give an overview of the current state of the art in the field of polydisperse phase equilibria, focusing on theoretical approaches for predicting coexistence between bulk phases. Polydisperse systems are characterized by an effectively infinite number of distinguishable particle species (and thus of conserved densities), and this makes even the apparently simple task of predicting phase equilibria from a known free energy (functional) highly non-trivial. As reviewed in section 3, a number of methods have been developed to tackle this problem; the most detailed understanding of phase behaviour can be achieved for truncatable free energies, whose excess part depends only on a number of moments of the density distribution $\rho(\sigma)$ rather than on all its details. As shown in section 4, many (approximate) free energies that can be used to describe polymeric and colloidal system fall into this class. The phase behaviour that even these relatively simple models produce is extremely rich compared to that of monodisperse systems, and many intriguing questions remain unanswered. The same is true, to an even greater degree, of the largely unexplored areas of interfacial behaviour and phase separation kinetics which I touched on briefly in section 5.

Acknowledgments

I have greatly benefited from stimulating and helpful discussions with M E Cates, N Clarke, R M L Evans, T C B McLeish, P Olmsted, I Pagonabarraga, W C K Poon, R Sear, A Speranza, and P B Warren; I also acknowledge partial financial support from EPSRC (GR/R52121/01).

References

[1] Cates M E and Candau S J 1990 Statics and dynamics of wormlike surfactant micelles *J. Phys.: Condens. Matter* **2** 6869–92

[2] Stapleton M R, Tildesley D J, Sluckin T J and Quirke N 1988 Computer-simulation of polydisperse liquids with density-dependent and temperature-dependent distributions *J. Phys. Chem.* **92** 4788–96

[3] Stapleton M R, Tildesley D J and Quirke N 1990 Phase-equilibria in polydisperse fluids *J. Chem. Phys.* **92** 4456–67

[4] Blaak R and Cuesta J A 2001 Continuous phase transition in polydisperse hard-sphere mixture *J. Chem. Phys.* **115** 963–9

[5] de Donder Th 1927 *L'Affinité* (Paris: Gauthier-Villars)

[6] Flory P J 1944 Thermodynamics of heterogeneous polymers and their solutions *J. Chem. Phys.* **12** 425–38

[7] Scott R L and Magat M 1945 The thermodynamics of high polymer solutions: 1. The free energy of mixing of solvents and polymers of heterogeneous distribution *J. Chem. Phys.* **13** 172–7

[8] Scott R L 1945 The thermodynamics of high polymer solutions: 2. The solubility and fractionation of a polymer of heterogeneous distribution *J. Chem. Phys.* **13** 178–87

[9] Scott R L 1952 Thermodynamics of high polymer solutions. 6. The compatibility of copolymers *J. Polym. Sci.* **9** 423–32

[10] Koningsveld R and Staverman A J 1967 *Kolloid Z. Z. Polym.* **218** 114

[11] Koningsveld R and Staverman A J 1967 *Kolloid Z. Z. Polym.* **220** 31

[12] Koningsveld R and Staverman A J 1968 *J. Polym. Sci.* A2 **6** 325

[13] Solc K 1970 Cloud-point curves of polymer solutions *Macromolecules* **3** 665–73

[14] Bowman J R 1949 Distillation of an indefinite number of components *Indust. Eng. Chem.* **41** 2004–7

[15] Hoffman E J 1968 Flash calculations for petroleum fractions *Chem. Eng. Sci.* **23** 957

[16] Blum L and Stell G 1979 Polydisperse systems. I. Scattering function for polydisperse fluids of hard or permeable spheres *J. Chem. Phys.* **71** 42–6

[17] Dickinson E 1980 Statistical thermodynamics of fluid phase equilibrium in a conformal polydisperse system *J. Chem. Soc. Faraday Trans.* II **76** 1458–67

[18] Flory P J and Abe A 1978 Statistical thermodynamics of mixtures of rodlike particles *Macromolecules* **11** 1119

[19] DeHoff R T 1992 *Thermodynamics in Material Science* (New York: McGraw-Hill)

[20] Salacuse J J and Stell G 1982 Polydisperse systems—statistical thermodynamics, with applications to several models including hard and permeable spheres *J. Chem. Phys.* **77** 3714–25

[21] Koningsveld R 1969 Phase relationships and fractionation in multicomponent polymer solutions *Pure Appl. Chem.* **20** 271–307

[22] Brannock G R 1991 Heterogeneous and homogeneous critical-points of polymer distributions *J. Chem. Phys.* **95** 612–27

[23] Sollich P, Warren P B and Cates M E 2001 Moment free energies for polydisperse systems *Adv. Chem. Phys.* **116** 265–336

[24] Rätzsch M T and Wohlfarth C 1991 Continuous thermodynamics of copolymer systems *Adv. Polym. Sci.* **98** 49–114

[25] Salacuse J J 1984 Random-systems of particles—an approach to polydisperse systems *J. Chem. Phys.* **81** 2468–81

[26] Warren P B 1998 Combinatorial entropy and the statistical mechanics of polydispersity *Phys. Rev. Lett.* **80** 1369–72

[27] Gualtieri J A, Kincaid J M and Morrison G 1982 Phase-equilibria in polydisperse fluids *J. Chem. Phys.* **77** 521–36

[28] Michelsen M L 1982 The isothermal flash problem. Part 1. Stability. *Fluid Phase Equilib.* **9** 1–19

[29] Cuesta J A 1999 Demixing in a single-peak distributed polydisperse mixture of hard spheres *Europhys. Lett.* **46** 197–203

[30] Fisher M E and Zinn S 1998 The shape of the van der Waals loop and universal critical amplitude ratios *J. Phys. A: Math. Gen.* **31** L629–35

[31] Hendriks E M 1987 Simplified phase-equilibrium equations for multicomponent systems *Fluid Phase Equilib.* **33** 207–21

[32] Hendriks E M 1988 Reduction theorem for phase-equilibrium problems *Indust. Eng. Chem. Res.* **27** 1728–32

[33] Hendriks E M and Vanbergen A R D 1992 Application of a reduction method to phase-equilibria calculations *Fluid Phase Equilib.* **74** 17–34

[34] Press W H, Teukolsky S A, Vetterling W T and Flannery B P 1992 *Numerical Recipes in C* 2nd edn (Cambridge: Cambridge University Press)

[35] Gordon M, Irvine P and Kennedy J W 1977 Phase diagrams and pulse-induced critical scattering *J. Polym. Sci.: Polym. Symp.* **61** 199–220
[36] Irvine P and Gordon M 1981 Truncation theorems for spinodals and critical-points of mean-field models for polydisperse polymer-solutions *Proc. R. Soc.* A **375** 397–408
[37] Beerbaum S, Bergmann J, Kehlen H and Rätzsch M T 1986 Spinodal equation for polydisperse polymer-solutions *Proc. R. Soc.* A **406** 63–73
[38] Warren P B 1999 Fluid–fluid phase separation in hard spheres with a bimodal size distribution *Europhys. Lett.* **46** 295–300
[39] Beerbaum S, Bergmann J, Kehlen H and Rätzsch M T 1987 Critical-point equations for polydisperse polymer-solutions *Proc. R. Soc.* A **414** 103–10
[40] Bauer B J 1985 Equilibrium phase compositions of heterogeneous copolymers *Polym. Eng. Sci.* **25** 1081–7
[41] Nesarikar A, Olvera de la Cruz M and Crist B 1993 Phase-transitions in random copolymers *J. Chem. Phys.* **98** 7385–97
[42] Solc K 1993 Phase-separation in bulk statistical copolymers and their mixtures with homopolymers. 1: Theory *Makromol. Chem.–Macromol. Symp.* **70+711** 93–105
[43] Solc K and Koningsveld R 1995 Liquid–liquid phase-separation in multicomponent polymer systems. 26. Blends of 2 polydisperse polymers *Coll. Czech. Chem. Commun.* **60** 1689–718
[44] Clarke N, McLeish T C B and Jenkins S D 1995 Phase-behavior of linear branched polymer blends *Macromol.* **28** 4650–9
[45] Henley E J and Rosen E M 1969 *Material and Energy Balance Computation* (New York: Wiley)
[46] Prausnitz J M, Anderson T F, Grens E A, Echert C A, Hsieh R and O'Connell J P 1980 *Computer Calculations for Multicomponent Vapor–Liquid and Liquid–Liquid Equilibria* (Englewood Cliffs, NJ: Prentice-Hall)
[47] Michelsen M L 1994 Calculation of multiphase equilibrium *Comput. Chem. Eng.* **18** 545–50
[48] Michelsen M L 1982 The isothermal flash problem. Part 2. Phase-split calculation *Fluid Phase Equilib.* **9** 21–40
[49] Michelsen M L 1986 Simplified flash calculations for cubic equations of state *Indust. Eng. Chem. Proc. Des. Dev.* **25** 184–8
[50] Michelsen M L 1993 Phase-equilibrium calculations—what is easy and what is difficult *Comput. Chem. Eng.* **17** 431–9
[51] Heidemann R A and Michelsen M L 1995 Instability of successive substitution *Indust. Eng. Chem. Res.* **34** 958–66
[52] Michelsen M L 1994 A simple method for calculation of approximate phase boundaries *Fluid Phase Equilib.* **98** 1–11
[53] Nakata M, Dobashi T, Inakuma Y and Yamamura K 1999 Coexistence curve of polystyrene in methylcyclohexane. X. Two-phase coexistence curves for ternary solutions near the tricritical compositions *J. Chem. Phys.* **111** 6617–24
[54] Cotterman R L and Prausnitz J M 1985 Flash calculations for continuous or semicontinuous mixtures using an equation of state *Indust. Eng. Chem. Proc. Des. Dev.* **24** 434–43
[55] Shibata S K, Sandler S I and Behrens R A 1987 Phase-equilibrium calculations for continuous and semicontinuous mixtures *Chem. Eng. Sci.* **42** 1977–88
[56] Daguanno B and Klein R 1992 Integral-equation theory of polydisperse Yukawa systems *Phys. Rev.* A **46** 7652–6
[57] Drohm J K and Schlijper A G 1986 Vapor–liquid equilibrium calculations by constrained free energy minimization *Int. J. Thermophys.* **7** 407–19
[58] Irvine P A and Kennedy J W 1982 Efficient computation of phase-equilibria in polydisperse polymer-solutions using R-equivalent delta-function molecular-weight distributions *Macromolecules* **15** 473–82
[59] Cotterman R L, Bender R and Prausnitz J M 1985 Phase-equilibria for mixtures containing very many components—development and application of continuous thermodynamics for chemical process design *Indust. Eng. Chem. Proc. Des. Dev.* **24** 194–203
[60] Du P C and Mansoori G A 1987 Phase-equilibrium of multicomponent mixtures—continuous mixture Gibbs free energy minimization and phase rule *Chem. Eng. Commun.* **54** 139–48
[61] Mansoori G A, Du P C and Antoniades E 1989 Equilibrium in multiphase polydisperse fluids *Int. J. Thermophys.* **10** 1181–204
[62] Kincaid J M, Shon K B and Fescos G 1989 New methods for calculating the dew bubble curves of classical model fluids *J. Stat. Phys.* **57** 937–63
[63] Kincaid J M, Morrison G and Lindeberg E 1983 Phase-equilibrium in nearly monodisperse fluids *Phys. Lett.* A **96** 471–4
[64] Briano J G and Glandt E D 1984 Statistical thermodynamics of polydisperse fluids *J. Chem. Phys.* **80** 3336–43
[65] Evans R M L, Fairhurst D J and Poon W C K 1998 Universal law of fractionation for slightly polydisperse

systems *Phys. Rev. Lett.* **81** 1326–9
[66] Evans R M L 1999 Fractionation of polydisperse systems: multiphase coexistence *Phys. Rev.* E **59** 3192–5
[67] Evans R M L 2001 Perturbative polydispersity: phase equilibria of near-monodisperse systems *J. Chem. Phys.* **114** 1915–31
[68] Xu H and Baus M 2000 Density functional theory of phase coexistence in weakly polydisperse fluids *Phys. Rev.* E **61** 3249–51
[69] Sollich P and Cates M E 1998 Projected free energies for polydisperse phase equilibria *Phys. Rev. Lett.* **80** 1365–8
[70] Clarke N, Cuesta J A, Sear R, Sollich P and Speranza A 2000 Phase equilibria in the polydisperse Zwanzig model of hard rods *J. Chem. Phys.* **113** 5817–29
[71] Michelsen M L 1987 Multiphase isenthalpic and isentropic flash algorithms *Fluid Phase Equilib.* **33** 13–27
[72] Michelsen M L 1986 Some aspects of multiphase calculations *Fluid Phase Equilib.* **30** 15–29
[73] Flory P J 1953 *Principles of Polymer Chemistry* (Ithaca, NY: Cornell University Press)
[74] Tompa H 1949 *Trans. Faraday Soc.* **45** 1142
[75] Tompa H 1956 *Polymer Solutions* (London: Butterworth)
[76] Solc K, Kleintjens L A and Koningsveld R 1984 Multiphase equilibria in solutions of polydisperse homopolymers. 3: Multiple critical-points *Macromolecules* **17** 573–85
[77] Dobashi T and Nakata M 1986 Coexistence curve of polystyrene in methylcyclohexane: 4. 3-phase coexistence curve of ternary-system *J. Chem. Phys.* **84** 5775–81
[78] Nakata M and Dobashi T 1986 Coexistence curve of polystyrene in methylcyclohexane: 5. Critical-behavior of the 3-phase coexistence curve *J. Chem. Phys.* **84** 5782–6
[79] Sundar G and Widom B 1988 Three-phase equilibrium in solutions of polystyrene homologues in cyclohexane *Fluid Phase Equilib.* **40** 289–303
[80] Shen W, Smith G R, Knobler C M and Scott R L 1990 Tricritical phenomena in bimodal polymer-solutions—3-phase coexistence curves for the system polystyrene (1) + polystyrene (2) + methylcyclohexane *J. Phys. Chem.* **94** 7943–9
[81] Solc K and Battjes K 1985 Multiphase equilibria in solutions of polydisperse homopolymers: 4. 3-phase and 4-phase separations in quaternary systems *Macromolecules* **18** 220–31
[82] Suzuki M, Dobashi T, Mikawa Y, Yamamura K and Nakata M 2000 Reentrant three-phase equilibrium of homologous polystyrene solution *J. Phys. Soc. Japan* **69** 1741–4
[83] Solc K 1975 Cloud-point curves of polymers with logarithmic-normal distribution of molecular weight *Macromol.* **8** 819–27
[84] de Loos T W, Poot W and Diepen G A M 1983 Fluid phase-equilibria in the system polyethylene + ethylene: 1. Systems of linear polyethylene + ethylene at high-pressure *Macromolecules* **16** 111–7
[85] Kita R, Dobashi T, Yamamoto T, Nakata M and Kamide K 1997 Coexistence curve of a polydisperse polymer solution near the critical point *Phys. Rev.* E **55** 3159–63
[86] Leibler L 1981 Theory of phase-equilibria in mixtures of co-polymers and homopolymers: 1. Phase-diagram *Makromol. Chem.–Rapid Commun.* **2** 393–400
[87] Broseta D and Fredrickson G H 1990 Phase-equilibria in copolymer–homopolymer ternary blends—molecular-weight effects *J. Chem. Phys.* **93** 2927–38
[88] Rätzsch M T, Kehlen H and Browarzik D 1985 Liquid–liquid equilibrium of polydisperse copolymer solutions—multivariate distribution-functions in continuous thermodynamics *J. Macromol. Sci.* A **22** 1679–90
[89] Rätzsch M T, Kehlen H, Browarzik D and Schirutschke M 1986 Cloud-point curve for the system copoly(ethylene-vinyl acetate) plus methyl acetate—measurement and prediction by continuous thermodynamics *J. Macromol. Sci. Chem.* A **23** 1349–61
[90] Rätzsch M T, Browarzik D and Kehlen H 1989 Refined continuous thermodynamic treatment for the liquid–liquid equilibrium of copolymer solutions *J. Macromol. Sci. Chem.* A **26** 903–20
[91] Bellier-Castella L, Xu H and Baus M 2000 Phase diagrams of polydisperse van der Waals fluids *J. Chem. Phys.* **113** 8337–47
[92] Bellier-Castella L, Baus M and Xu H 2001 Three-phase fractionation of polydisperse fluids *J. Chem. Phys.* **115** 3381–6
[93] Sollich P 2002 in preparation
[94] Pusey P N and van Megen W 1986 Phase-behavior of concentrated suspensions of nearly hard colloidal spheres *Nature* **320** 340–2
[95] Pusey P N 1991 *Liquids, Freezing and Glass Transitions (Les Houches Session LI) (NATO ASI Series B: Physics)* ed J-P Hansen, D Levesque and J Zinn-Justin (Amsterdam: North-Holland) ch 10
[96] Pusey P N and van Megen W 1987 Observation of a glass-transition in suspensions of spherical colloidal particles *Phys. Rev. Lett.* **59** 2083–6

[97] Evans R M L and Holmes C B 2001 Diffusive growth of polydisperse hard-sphere crystals *Phys. Rev.* E **6401** 1404−+ (article No 011404)
[98] Zhu J X, Li M, Rogers R, Meyer W, Ottewill R H, Russell W B and Chaikin P M 1997 Crystallization of hard-sphere colloids in microgravity *Nature* **387** 883–5
[99] Phan S E, Russel W B, Zhu J X and Chaikin P M 1998 Effects of polydispersity on hard sphere crystals *J. Chem. Phys.* **108** 9789–95
[100] Dickinson E and Parker R 1985 Polydispersity and the fluid–crystalline phase-transition *J. Physique Lett.* **46** L229–32
[101] Pusey P N 1987 The effect of polydispersity on the crystallization of hard spherical colloids *J. Physique* **48** 709–12
[102] McRae R and Haymet A D J 1988 Freezing of polydisperse hard-spheres *J. Chem. Phys.* **88** 1114–25
[103] Barrat J L and Hansen J-P 1986 On the stability of polydisperse colloidal crystals *J. Physique* **47** 1547–53
[104] Bolhuis P G and Kofke D A 1996 Monte Carlo study of freezing of polydisperse hard spheres *Phys. Rev.* E **54** 634–43
[105] Kofke D A and Bolhuis P G 1999 Freezing of polydisperse hard spheres *Phys. Rev.* E **59** 618–22
[106] Almarza N G and Enciso E 1999 Freezing of polydisperse hard spheres *Preprint* cond-mat/9905282
[107] Sear R P 1999 Depletion-induced demixing in polydisperse mixtures of hard spheres *Phys. Rev. Lett.* **82** 4244–7
[108] Wilding N B and Sollich P 2001 Grand canonical ensemble simulation studies of polydisperse fluids *J. Chem. Phys.* submitted
(Wilding N B and Sollich P 2001 Grand canonical ensemble simulation studies of polydisperse fluids *Preprint* cond-mat/0111274)
[109] Boublik T 1970 *J. Chem. Phys.* **53** 471
[110] Mansoori G A, Carnahan N F, Starling K E and Leland T W Jr 1971 *J. Chem. Phys.* **54** 1523
[111] Bartlett P 1999 Thermodynamic properties of polydisperse hard spheres *Mol. Phys.* **97** 685–93
[112] Gazzillo D, Giacometti A and Carsughi F 1997 Scattering functions for multicomponent mixtures of charged hard spheres, including the polydisperse limit: analytic expressions in the mean spherical approximation *J. Chem. Phys.* **107** 10 141–53
[113] Tutschka C and Kahl G 1998 The mean spherical model for a Lorentz–Berthelot mixture of sticky hard spheres *J. Chem. Phys.* **108** 9498–505
[114] Gazzillo D and Giacometti A 2000 Structure factors for the simplest solvable model of polydisperse colloidal fluids with surface adhesion *J. Chem. Phys.* **113** 9837–48
[115] Tutschka C and Kahl G 2001 Thermodynamic properties of a polydisperse system *Phys. Rev.* E **64** 031104
[116] Sear R P 1998 Phase separation and crystallisation of polydisperse hard spheres *Europhys. Lett.* **44** 531–5
[117] Bartlett P 1997 A geometrically-based mean-field theory of polydisperse hard-sphere mixtures *J. Chem. Phys.* **107** 188–96
[118] Bartlett P and Warren P B 1999 Reentrant melting in polydispersed hard spheres *Phys. Rev. Lett.* **82** 1979–82
[119] Bartlett P 1998 Fractionated crystallization in a polydisperse mixture of hard spheres *J. Chem. Phys.* **109** 10 970–5
[120] Ilett S M, Orrock A, Poon W C K and Pusey P N 1995 Phase-behavior of a model colloid–polymer mixture *Phys. Rev.* E **51** 1344–52
[121] Lekkerkerker H N W, Poon W C K, Pusey P N, Stroobants A and Warren P B 1992 Phase-behavior of colloid plus polymer mixtures *Europhys. Lett.* **20** 559–64
[122] Dijkstra M, Brader J M and Evans R 1999 Phase behaviour and structure of model colloid–polymer mixtures *J. Phys.: Condens. Matter* **11** 10 079–106
[123] Asakura S and Oosawa F 1954 *J. Chem. Phys.* **22** 1255
[124] Warren P B, Ilett S M and Poon W C K 1995 Effect of polymer nonideality in a colloid–polymer mixture *Phys. Rev.* E **52** 5205–13
[125] Sear R P and Frenkel D 1997 Phase behavior of colloid plus polydisperse polymer mixtures *Phys. Rev.* E **55** 1677–81
[126] Lee J T and Robert M 1999 Phase transitions of colloid–polymer systems in two dimensions *Phys. Rev.* E **60** 7198–202
[127] Warren P B 1997 Phase behavior of a colloid plus binary polymer mixture: theory *Langmuir* **13** 4588–94
[128] Fairhurst D J 1999 Polydispersity in colloidal phase transitions *PhD Thesis* University of Edinburgh, UK
[129] Maier W and Saupe A 1958 *Z. Naturf.* a **13** 564
[130] Sluckin T J 1989 Polydispersity in liquid-crystal systems *Liquid Crystals* **6** 111–31
[131] Speranza A and Sollich P 2002 in preparation
[132] Onsager L 1949 *Ann. NY. Acad. Sci.* **51** 627
[133] Buining P A and Lekkerkerker H N W 1993 Isotropic–nematic phase-separation of a dispersion of organophilic

boehmite rods *J. Phys. Chem.* **97** 11 510–6
[134] Vroege G J and Lekkerkerker H N W 1992 Phase-transitions in lyotropic colloidal and polymer liquid-crystals *Rep. Prog. Phys.* **55** 241–1309
[135] Lekkerkerker H N W, Coulon P, van der Haegen R and Deblieck R 1984 On the isotropic–liquid crystal phase-separation in a solution of rodlike particles of different lengths *J. Chem. Phys.* **80** 3427–33
[136] Odijk T and Lekkerkerker H N W 1985 Theory of the isotropic–liquid-crystal phase-separation for a solution of bidisperse rodlike macromolecules *J. Phys. Chem.* **89** 2090–6
[137] Vroege G J and Lekkerkerker H N W 1993 Theory of the isotropic–nematic phase-separation for a solution of bidisperse rodlike particles *J. Phys. Chem.* **97** 3601–5
[138] van Roij R and Mulder B 1996 Absence of high-density consolute point in nematic hard rod mixtures *J. Chem. Phys.* **105** 11 237–45
[139] Hemmer P C 1999 Phase transitions in a solution of rodlike macromolecules of two different sizes *Mol. Phys.* **96** 1153–7
[140] Vroege G J and Lekkerkerker H N W 1997 Theory of phase separation for a solution of tridisperse rod-like particles *Colloids Surf.* A **130** 405–13
[141] Sear R P and Jackson G 1995 Theory for the phase-behavior of a mixture of a rodlike colloid and a rodlike polymer *J. Chem. Phys.* **103** 8684–93
[142] van Roij R, Mulder B and Dijkstra M 1998 Phase behavior of binary mixtures of thick and thin hard rods *Physica* A **261** 374–90
[143] Chen Z Y 1994 Effect of polydispersity on the isotropic–nematic phase-transition of rigid rods *Phys. Rev.* E **50** 2849–55
[144] Clarke N and McLeish T C B 1992 Phase-behavior of a binary mixture of long thin rods *J. Physique* II **2** 1841–52
[145] Kayser R F and Raveche H J 1978 *Phys. Rev.* A **17** 2067
[146] Bates M A and Frenkel D 1998 Influence of polydispersity on the phase behavior of colloidal liquid crystals: a Monte Carlo simulation study *J. Chem. Phys.* **109** 6193–9
[147] Bohle A M, Holyst R and Vilgis T 1996 Polydispersity and ordered phases in solutions of rodlike macromolecules *Phys. Rev. Lett.* **76** 1396–9
[148] Martinez-Raton Y, Cuesta J A, van Roij R and Mulder B 1999 Nematic to smectic: a 'hard' transition *New Approaches to Problems in Liquid State Theory* ed C Caccamo (Kluwer: Academic) pp 139–50
[149] van Roij R and Mulder B 1996 Demixing versus ordering in hard-rod mixtures *Phys. Rev.* E **54** 6430–40
[150] van der Kooij F M and Lekkerkerker H N W 1998 Formation of nematic liquid crystals in suspensions of hard colloidal platelets *J. Phys. Chem.* B **102** 7829–32
[151] Bates M A and Frenkel D 1999 Nematic–isotropic transition in polydisperse systems of infinitely thin hard platelets *J. Chem. Phys.* **110** 6553–9
[152] van der Kooij F M, Vogel M and Lekkerkerker H N W 2000 Phase behavior of a mixture of platelike colloids and nonadsorbing polymer *Phys. Rev.* E **62** 5397–402
[153] van der Kooij F M, Kassapidou K and Lekkerkerker H N W 2000 Liquid crystal phase transitions in suspensions of polydisperse plate-like particles *Nature* **406** 868–71
[154] van der Kooij F M and Lekkerkerker H N W 2000 Liquid-crystalline phase behavior of a colloidal rod-plate mixture *Phys. Rev. Lett.* **84** 781–4
[155] van der Kooij F M and Lekkerkerker H N W 2000 Liquid-crystal phases formed in mixed suspensions of rod- and platelike colloids *Langmuir* **16** 10 144–9
[156] Evans R 1992 *Fundamentals of Inhomogeneous Fluids* ed D Henderson (New York: Dekker) p 85
[157] Lowen H 1994 Melting, freezing and colloidal suspensions *Phys. Rep.* **237** 249–324
[158] Pagonabarraga I, Cates M E and Ackland G J 2000 Local size segregation in polydisperse hard sphere fluids *Phys. Rev. Lett.* **84** 911–4
[159] Warren P B 1999 Phase transition kinetics in polydisperse systems *Phys. Chem. Chem. Phys* **1** 2197–202
[160] Pagonabarraga I and Cates M E 2001 A practical density functional for polydisperse polymers *Europhys. Lett.* **55** 348–54
[161] Clarke N 2001 Early stages of phase separation from polydisperse polymer mixtures *Eur. Phys. J.* E **4** 327–36